Review of Fiber-Optic Localized Surface Plasmon Resonance Sensors: Geometries, Fabrication Technologies, and Bio-Applications

Mengdi LU[1,2*], Chen WANG[2], Ruizhi FAN[2], Ming LIN[2], Jianye GUANG[2], and Wei PENG[2]

[1]*Affiliated Cancer Hospital, Dalian University of Technology, Shenyang 110042, China*

[2]*School of Physics, Dalian University of Technology, Dalian 116024, China*

*Corresponding author: Mengdi LU   E-mail: mdlu@dlut.edu.cn

Abstract: Localized surface plasmon resonance (LSPR) biosensors, which enable nanoscale confinement and manipulation of light, offer the enhanced sensitivity and electromagnetic energy localization. The integration of LSPR with the fiber-optic technology has led to the development of compact and versatile sensors for miniaturization and remote sensing. This comprehensive review explores various sensor configurations, fiber types, and geometric shapes, highlighting their benefits in terms of sensitivity, integration, and performance improvement. Fabrication techniques such as focused non-chemical bonding strategies and self-assembly of nanoparticles are discussed, providing control over nanostructure morphology and enhancing sensor performance. Bio-applications of fiber-optic LSPR (FOLSPR) sensors are detailed, specifically in biomolecular interactions and analysis of proteins, pathogens and cells, nucleic acids (DNA and RNA), and other small molecules (organic compounds and heavy metal ions). Surface modification and detection schemes are emphasized for their potential for label-free and real-time biosensing. The challenges and prospects of FOLSPR sensors are addressed, including the developments in sensitivity, fabrication techniques, and measurement reliability. Integration with emerging technologies such as nanomaterials is highlighted as a promising direction for future research. Overall, this review provides insights into the advancements and potential applications of FOLSPR sensors, paving the way for sensitive and versatile optical biosensing platforms in various fields.

Keywords: Fiber-optic; localized surface plasmon resonance; biosensor; nanoparticles; geometric configuration; fabrication technology

1. Introduction

Surface plasmons are collective electron oscillations that occur at the interface between a metal and a dielectric, resulting in the generation of surface plasmon polaritons upon excitation by light [1]. This phenomenon is influenced by the properties of the materials and the incident light, allowing for the confinement and manipulation of light at the nanoscale [2]. Through the coupling of

the oscillating electric field of the incident light with the collective motion of electrons on the metal surface, surface plasmons can propagate along the metal-dielectric interface, leading to significant field enhancements and the localization of the electromagnetic energy. When the incident light matches the wavevector of the surface plasmons, a dip in the intensity of the reflected or transmitted light, known as the surface plasmon resonance (SPR) dip, can be observed [3]. This dip is highly sensitive to changes in the refractive index (RI) of the surrounding medium. Consequently, surface plasmons have found extensive application in label-free and real-time detection of biomolecular interactions [4], such as DNA hybridization and antibody-antigen recognition, enabling nanoscale analysis of chemical and biological interactions through the unique properties of plasmonic materials [5]. Localized surface plasmon resonance (LSPR) is a variation of the SPR that occurs in nanostructures, such as nanoparticles or periodic arrays, which possess distinctive plasmonic properties [6]. In contrast to the SPR, which relies on macroscopic surfaces, the LSPR can be customized by controlling the size, shape, and composition of the nanostructures, allowing for tunability of the resonance wavelengths and enhanced sensitivity [7]. Consequently, LSPR sensors are highly attractive for various applications, including bio-sensing, environmental monitoring, and nanophotonics [8]. The integration of the fiber-optic technology with the LSPR has resulted in the development of compact and versatile sensors, facilitating miniaturization, and remote sensing. These advancements have opened up new possibilities for highly sensitive and compact optical sensing in various fields. Fiber-optic based sensors have gained attention for their small size, high sensitivity, compatibility with remote and real-time monitoring, and the potential for multiplexed measurements [9].

This review aims to provide a comprehensive overview of fiber-optic LSPR (FOLSPR) sensors,

with a focus on their configurations, types, geometries, fabrication technologies, and bio-applications. FOLSPR sensors can be classified into two primary categories: straight transmissive and flatheaded reflective configurations. Both configurations offer distinct advantages and can be tailored to specific sensing requirements, depending on factors, such as the desired sensitivity, measurement setup, and experimental conditions [10]. Different fiber types, such as single-mode fibers (SMFs), multimode fibers (MMFs), photonic crystal fibers (PCFs), and specialty fibers [e.g., microfibers and fiber Bragg gratings (FBGs)], can be used in these configurations, each offering unique advantages in terms of sensitivity, flexibility, and integration with other systems. The geometric shapes employed in FOLSPR sensors also play a significant role in enhancing their performance. LSPR biosensors with special geometries, including tapered, U-type, Ω-type, and D-type shapes, effectively enhance the sensitivity of the sensors and meet specific assembly requirements of subsequent sensing structures. Furthermore, this review will delve into the different fabrication technologies utilized in the development of FOLSPR sensors. These techniques include top-down fabrication of periodic nanostructures using the focused ion beam (FIB) or electron beam lithography (EBL), surface self-assembly of nanoparticles, and bottom-up nanostructured film transfer techniques [11, 12]. These fabrication technologies allow for precise control over the surface morphology of the nanostructures, further enhancing the performance of the sensors. In addition, the diverse bio-applications of FOLSPR sensors are also explored, including their utilization in the detection and analysis of biomolecules, such as proteins, DNA, and viruses [13]. Specific surface modification and detection schemes will be discussed in detail. The potential applications of FOLSPR sensors in medical diagnostics, environmental monitoring, and food safety will also be investigated [14]. It should

be noted that the challenges and prospects in the development of FOLSPR sensors will also be highlighted. These challenges include improving the sensor sensitivity, optimizing the fabrication techniques, and enhancing the reliability and reproducibility of sensor measurements. Potential areas of future research and advancements, such as the integration of FOLSPR sensors with technologies like nanomaterials, will also be outlined.

Overall, the purpose of this review is to provide a comprehensive understanding of FOLSPR sensors, their fabrication techniques, and their wide range of bio-applications. By exploring different geometries, fabrication technologies, and potential applications, this review aims to contribute to the advancement and adoption of FOLSPR sensors in fields such as human health, drug screening, food safety, and environmental monitoring.

2. Geometric configurations of FOLSPR sensors

FOLSPR sensors have been widely used for sensitive detection and analysis of biochemical reactions. The LSPR phenomenon occurs when light interacts with nanoscale metal structures, resulting in a spectral shift in the resonance frequency that is sensitive to the RI changes in the surrounding medium. In order to increase the sensitivity, selectivity, and versatility of LSPR sensors, the geometric configuration of the fiber probe has been continuously modified. Typically, the LSPR sensing performance can be effectively achieved by using different types of optical fibers, optimizing the geometric structure of the fiber probe, and adopting different optical transmission modes. These geometries provide unique advantages in terms of sensitivity, stability, and multiplexing capabilities, depending on the specific design. Overall, the geometric configurations of FOLSPR sensors play a crucial role in determining the sensing performance and enabling practical applications in biomedical

sensing, environmental monitoring, and chemical analysis.

2.1 Propagation path of light

The LSPR phenomenon for fiber-optic sensors is produced by the interaction between light and metallic nanoparticles or nanoarrays immobilized on the fiber. The LSPR effect occurs when the incident light matches the resonance frequency of the nanostructures in the evanescent field, resulting in a strong absorption or scattering of the light. This interaction is determined by the plasmonic properties of the nanostructures and can be quantified using the Mie theory. By monitoring the spectral response of the scattered light, changes in the surrounding RI can be detected, enabling the sensitive detection of various analytes or environmental parameters.

There are two main configurations for FOLSPR sensors based on the propagation path of light: straight transmission [15] and flatheaded reflection [16]. Figure 1(a) illustrates the straight transmissive FOLSPR sensor setup. Incident light is coupled into one end of the fiber and propagates through the fiber core. The LSPR-active nanostructures are immobilized on the side-outer surface of the fiber as the sensing area. The light is then received by a signal-receiving device at the other end. As the light interacts with the nanostructures along the transmission path, the LSPR effect induces changes in the transmitted light intensity or wavelength, which can be measured at the output end. In contrast, as shown in Fig. 1(b), the flatheaded reflective configuration uses only one side of the fiber to transmit the incident light and also receives the end-face reflected signal through a fiber-optic coupler. The LSPR-active nanostructures are either immobilized on the fiber end-face or on the side-outer surface near the end of the fiber probe, while the reflected light from the sensing area is collected and analyzed to determine changes in the intensity or wavelength. The flatheaded reflective

configuration allows for easy integration with external systems, such as spectrometers or detectors, and is

suitable for applications where direct access to the sample is desired, such as in implantable medical diagnostics.
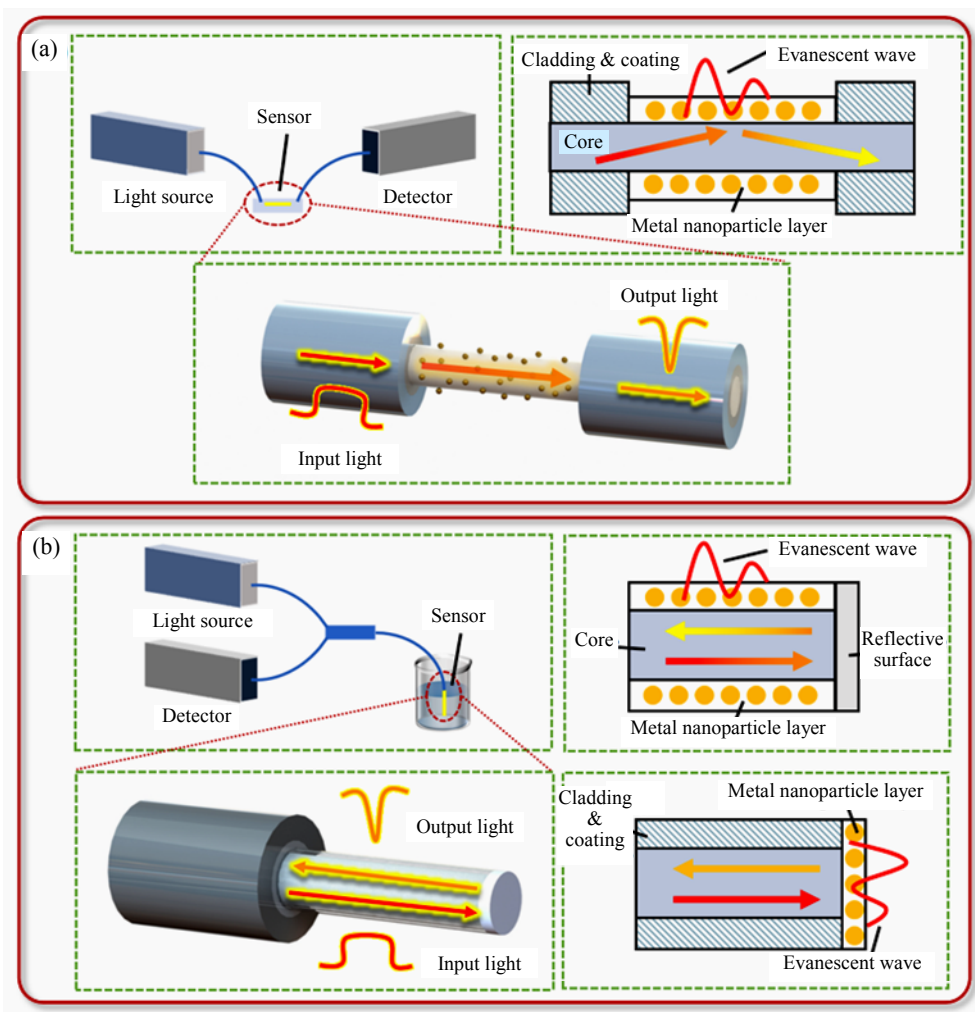

Fig. 1 Configurations of (a) straight transmissive and (b) flatheaded reflective FOLSPR sensors.

The choice between these two configurations depends on several factors. One crucial factor to consider is the characteristics of the sample being analyzed. For example, if the sample is sensitive to contact or requires a non-invasive approach, the straight transmission configuration would be more suitable as it allows for sensing over longer distances without direct contact with the sample. This is particularly advantageous in biological or hazardous environments. On the other hand, if direct access to the sample is desired, such as in implantable medical diagnostics, the flatheaded reflective configuration would be preferred. This configuration allows for easy integration with

external systems, such as spectrometers or detectors, enabling efficient analysis of the reflected light from the sensing area on the end-face or side-outer surface of the fiber probe. Another critical consideration when choosing the configuration is the specific sensing requirements. Both configurations can measure changes in the transmitted light intensity or wavelength induced by the LSPR effect. However, the straight transmission configuration may provide the better stability and repeatability due to the longer interaction path of light with the LSPR-active nanostructures along the fiber core. The flatheaded reflective configuration may offer the improved sensitivity in measurements, as it

relies on the precise collection of reflected light from the small bottom sensing area. Compatibility with the measurement setup is also an essential factor. The straight transmission configuration is relatively simpler, requiring a signal-receiving device at one end of the fiber to measure changes in transmitted light. The flatheaded reflective configuration with the additional Y-shaped fiber-optic coupler imposes higher requirements on the flatness of the fiber end face to ensure the satisfactory optical coupling efficiency.

2.2 Type of the optical fiber

Replacing the traditional prism with the optical fiber as the plasmonic element can overcome the limitations of the relatively bulky size, complex optics and mechanical structure, and inability for remote and on-site sensing. Additionally, it offers advantages such as the portability and implantable in situ detection. Since the first report of the fiber-based SPR sensor by R. C. Jorgenson and S. S. Yee [17] in 1993, various types of optical fibers as shown in Fig. 2 have been applied in plasmon resonance sensing, including SMFs, MMFs, hollow core fibers (HCFs), PCFs, micro/nano fibers (MNFs), and FBGs.

The traditional SMF and MMF are widely used due to their mature manufacturing processes. However, this type of sensor mainly realizes LSPR sensing by using the methods of core mismatch, reducing the thickness of the cladding, or using the fiber end face, since the evanescent field cannot penetrate the untreated large thickness cladding to excite the metal nanoparticles on the surface of the fiber to generate the LSPR. In Fig. 2(a), the SMF-LSPR sensor consists of an SMF with a nano-metallic layer, typically gold or silver, deposited on the declad fiber core as the sensing region. The metallic particle monolayer acts as a plasmonic nanostructure, which enhances the evanescent field interaction with the target analyte. The geometry can vary, including straight, tapered,

or U-shaped configurations, depending on the desired sensing outcomes. In comparison to other fiber structures, the SMF-LSPR sensor utilizes the evanescent field of a guided mode to interact with the analyte, providing compactness, simplicity, and compatibility with existing fiber-optic systems. However, the removal of the SMF cladding necessitates the use of strong acid etching or polishing procedures, which are both hazardous and complex. These processes also have the potential for resulting in uneven roughness on the sensing surface, subsequently reducing the sensitivity of the sensor. Otherwise, the MMF is the most widely used in LSPR sensors since it offers several advantages over the traditional SMF-LSPR sensor. The MMF allows for the propagation of multiple modes of light, resulting in enhanced sensing capabilities [Fig. 2(c)]. The common process of removing the plastic coating from the MMF only requires a simple physical stripping, without acid etching or polishing to damage the surface roughness of the fiber core. Compared to the SMF-LSPR sensor, this simplified process is advantageous in obtaining a more stable structure for sensing performance. Additionally, its larger core diameter facilitates the coupling of light to the sensor, making it more efficient and improving the signal-to-noise ratio.
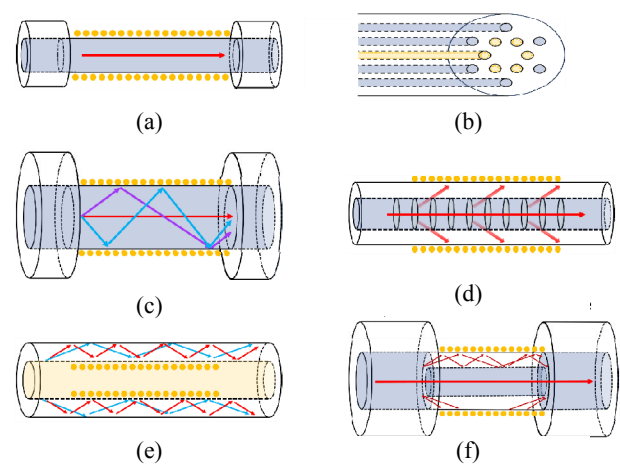
Fig. 2 Types of fiber optic (a) SMF, (b) PCF, (c) MMF, (d) FBG, (e) HCF, and (f) hetero-core structure fiber.

The HCF is a specialty fiber without a solid core structure. The sensing structure of HCF-LSPR sensors significantly differs from the others, as shown in Fig. 2(e). Besides being able to create a sensing region on the outer surface of the fiber, it also allows for the modification of metal nanoparticles on the inner wall of the HCF [18]. The unique structure of the HCF enables the internal air channel to also serve as the liquid flow channel [19]. This design helps to minimize the influence of the external environment on the liquid. Specially, for PCF-LSPR sensors in Fig. 2(b), the combination of the PCF with the LSPR can convert the transverse magnetic (TM) mode found in the traditional planar waveguides into hybrid modes. This transformation can be facilitated by adjusting the air holes-based structure of the PCF itself, allowing for easier phase matching between the core mode and the LSPR mode, and consequently generating the LSPR under specific wavelength conditions [20]. In addition, PCFs offer the advantages of the compact size and diverse internal air hole designs. The sensing region of these fibers can be configured to accommodate metal nanoparticles with diameters smaller than or significantly smaller than that of the air holes [21]. Alternatively, metal nanoparticles can be placed outside the PCF or selectively filled within part of the air holes [20, 22]. However, the fabrication process for filling the air holes presents huge challenges, and the detection range is limited. Therefore, the current research on PCF-LSPR sensors is predominantly in the theoretical analysis [23]. There is an ample scope for enhancing the structural design and detection stability.

Instead of removing a section of the cladding in order to access the core-guided light, gratings that have been photo-inscribed in the core can instead be utilized to diffract a portion of the light into the cladding [Fig. 2(d)]. Herein, the significant advantages utilizing the FBG are minimal impact on the mechanical resistance of the fiber and the coupling of gratings is a resonant phenomenon that only occurs at specific wavelengths in guided configurations. In other words, similar to a coupled resonator system, different fiber modes couple at different wavelengths where the grating couples two fiber modes and the metal particles layer couples a fiber mode to a localized surface plasmon polariton. When the two resonances overlap, the grating resonances become sensitive to changes in the LSPR. Due to modes coupling limitation, both long period fiber gratings (LPFGs) and tilted FBGs (TFBGs) can be directly used for the LSPR sensing, while the traditional short period fiber gratings require cladding removed. The FBG-based LSPR sensors [24] can provide the much narrower bandwidth compared to the conventional FOLSPR sensors (one-tenth or even one-hundredth of that in the MMF). However, it is challenging to excite the LSPR in the communication wavelength range using metal nanoparticles, necessitating the use of special designs such as nanowires or periodic arrays. The LPFGs based LSPR biosensor (operating in the visible spectral range) attains a limit of detection (LOD) low to $0.02\,\mu m$ for glyphosate [25]. The interaction of cysteamine and glyphosate leads to the change in the effective RI of LPFG cladding modes, causing a spectral shift in LPFG attenuation bands. The whole effect is based on the resonance between the LPFG attenuation bands and LSPR induced by nanoparticles, which increases the sensitivity. In addition, some strategies utilizing noble metal nanoparticles to enhance the sensing signals of TFBGs based sensors are also claimed as FOLSPR sensors. The surface modification of TFBGs with gold nanoparticles or gold nanocages can achieve a several-fold to several tens-fold enhancement in the detection sensitivity of molecules, such as proteins and glucose [26–28]. However, due to the significant difference in the excitation wavelengths between the detection spectral range (typically around $1500\,nm$) and LSPR of metal nanoparticles (typically in the visible light range), we personally prefer to refer to this strategy as the

localized electromagnetic field enhancement for sensing.

Currently, some special optical fibers or hetero-core fibers [Fig. 2(f)] are also used in the production of LSPR sensors. The MNF-based LSPR biosensor offers large fractions of evanescent fields and high surface field intensity, making it highly sensitive to disturbances in the surrounding medium, especially for the LSPR sensing structure [29]. The optimized MNF-based LSPR biosensor demonstrates the good capability for streptavidin detection with an LOD of 1 pg/mL [30]. P. Uebel *et al.* [31] proposed a gold-filled silica capillary and employed a wet-chemical etching and mechanical cleaving technique to fabricate gold nanotips attached to tapered optical fibers. This structure facilitates the creation of a plasmon-enhanced near-field fiber probe for the LSPR sensing. By adjusting the tip design, the resonance wavelength of the probe could be tuned within the range of 500 nm to 850 nm, exhibiting a small full width at half maximum (FWHM) of 90 nm. Besides, the hetero-core fibers such as MMF-SMF-MMF [32], MMF-PCF-MMF [33], PCF-FBG [34], and convex fiber-tapered seven-core fiber-convex fiber [35] splicing structures adopt the core mismatch scheme to realize high sensitivity external biomass sensing, and several typical hetero-core fibers based LSPR sensing structures are shown in Fig. 3. In 2008, B. T.

Wang *et al.* [36] proposed an MMF-PCF-MMF biosensor with a high RI sensitivity of 3 915 nm/RIU for human immunoglobulin G (IgG) detection. It uses both the SPR and LSPR principles by the coated gold film on the PCF section and nanoparticles monolayer attached to it. The LSPR excited by nanoparticles plays an important role in improving the sensitivity and reducing the LOD for biosensing. Recently, Y. Wang *et al.* [37] prepared the sensing structure of the MMF-photosensitive-MMF, following that, graphene oxide, gold nanoparticles (AuNPs), and molybdenum disulfide nanoparticles are immobilized to the etched structure surface to realize the LSPR biosensor for the detection of cardiac troponin I. A section of the multicore fiber comprising seven cores arranged in a hexagonal shape spliced with the SMF was employed as an LSPR biosensor for cancerous cells detection [Fig. 3(a)] [38]. The proposed sensor structure is etched in a controlled manner to increase the evanescent wave and coupling of modes between the cores of the multicore fiber. The sensitivity is further increased by immobilizing different nanomaterials, such as the optimized size of gold nanoparticles, graphene oxide, and copper oxide nanoflowers on the multicore fiber. The proposed etched sensor is ultra-sensitive for the detection of cancerous cells in a linear range of 10^2 cells/mL–10^6 cells/mL.
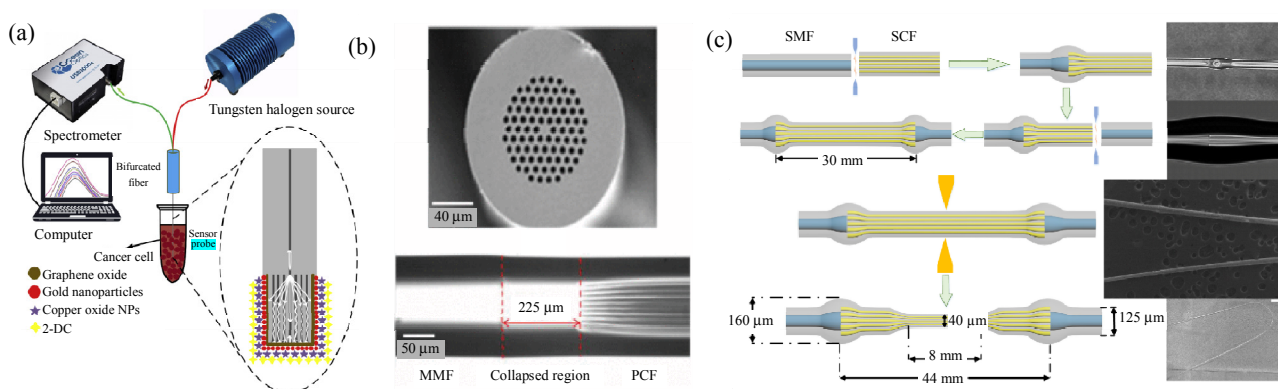

Fig. 3 Hetero-core fibers based LSPR sensing structures: (a) multicore fiber and SMF based structure [38], (b) MMF-PCF-MMF structure [36], and (c) convex fiber-tapered seven-core fiber-convex fiber structure [35].

2.3 Geometry of the optical fiber probe

Different from the methods of splicing several different types of optical fibers together, the method of appropriately modifying the geometric shape and structure of the optical fiber to improve the performance of LSPR fiber-optic biosensors has also attracted widespread attention. Based on their distinct shapes, LSPR biosensors with special geometries can be broadly categorized into several common types: the tapered, U-type, Ω-type, and D-type. Figure 3 illustrates the classification of LSPR biosensors with special geometries, along with examples of typical structures corresponding to each category.

The SMF has a strong ability to confine the incident light. The energy carried by higher-order modes leaks into the cladding as evanescent waves propagate. However, these higher-order modes carry very low energy and it is difficult to form a strong evanescent field [39]. Consequently, the intensity of the evanescent waves generated by the weak evanescent field is low, making the phenomenon of exciting the LSPR less obvious. In contrast, when the fiber is tapered as shown in Fig. 4(a), the ability of the core to confine light is greatly reduced, resulting in a huge change in the mode of the transmitted light. The energy of the transmitted light is coupled into the cladding, forming a strong evanescent field with a large penetration depth, which in turn excites the LSPR [30, 40]. There are three primary methods for fabricating tapered optical fibers: grinding [41], chemical etching [42], and fusion tapering [43, 44]. Among them, the grinding method is relatively primitive, only utilizing mechanical tools to polish and create a tapered shape but with higher mechanical strength. However, it suffers from poor repeatability and requires higher process accuracy. The chemical etching method is involved using a fluoride-based solvent with a specific ratio for corrosion. Despite its simplicity and cost-effectiveness, accurately controlling the taper angle proves challenging, leading to dispersion issues. In contrast, the fusion tapering method is the most efficient and widely employed technique for producing tapered fibers. It entails heating the fiber to a molten state using either a flame or arc discharge, followed by gradually tapering it under the applied tension. This approach facilitates precise control over the taper and shape, remains unaffected by external factors, and yields the greater repeatability and accuracy. Furthermore, researchers have expansively explored the SMF-LSPR sensors with various designs based on the single taper unit [43, 45, 46], including the periodically tapered structure, taper-in-taper structure, truncated semi-taper structure, and even serial quadruple tapered structure [47]. These sensing structures provide the higher sensitivity, however, as the number of tapers increases, the fiber becomes more fragile and easier to break than the original fiber structure, which needs to be further overcome.
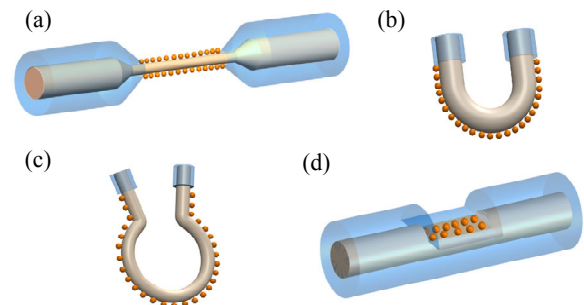

Fig. 4 Classification of LSPR biosensors with special geometries and typical structures: (a) tapered, (b) U-type, (c) Ω-type, and (d) D-type.

The structure of the U-shaped fiber LSPR sensor is shown in Fig. 4(b). By bending the sensing region into a U-shape, the angle of the light perpendicular to the core-cladding interface can be changed. To optimize and enhance the sensitivity, the outer bending radius can be adjusted. As the bending radius of the fiber decreases, the RI sensitivity increases. Once the radius decreases to a certain value, the sensitivity reaches its maximum. However, further decreasing the bending radius will result in a

reduction of the sensitivity. Therefore, exploring the optimal bending radius can effectively improve the sensitivity of the U-shaped fiber LSPR sensor. As early as 2009, V. V. R. Sai *et al*. [48] proposed a U-shaped LSPR sensor based on AuNPs. It is capable of detecting bulk refractive index changes with a sensitivity and a resolution of 540 nm/RIU and 3.8×10^{-5} RIU, respectively. The results obtained in biosensor applications are promising with a minimum LOD of 0.8 nM of anti-IgG. U-shaped fiber sensors are easy to fabricate and suitable for penetrating in some narrow gaps. However, they can easily break during the bending process, and the minimum bending diameter is limited, making it difficult to further enhance the sensing performance.

Based on the sensitivity enhancement principle of the U-shaped optical fiber sensor, in order to further increase the bending radius and bending length, S-shaped sensors have been proposed [49]. Compared to the single bending structure of the U-shaped sensor, the S-shaped sensor with two bending structures has the higher sensing sensitivity

due to the smaller bending radius and longer bending length. According to the experimental conclusion of S. K. Chauhan [50], the RI sensitivity of the S-shaped fiber is about 1.5 times that of the U-shaped fiber (Fig. 5). Although the S-shaped fiber has the higher sensitivity, its fragile structure with multiple bends makes it easily damaged by fast liquid flow, resulting in poor practicality. Furthermore, the Ω-shaped LSPR sensor [Fig. 4(c)] exhibits the enhanced performance when it has a smaller radius and a longer bending length, since the Ω-type fiber causes light attenuation in the bending part due to its interaction with the surrounding environment, resulting in the bending loss [51]. Among the other bent fibers, such as the U-shaped and S-shaped, the Ω-shaped fiber allows more fundamental modes to transfer from the fiber core into the cladding and induces a transition of the propagating mode from the fundamental mode to a higher-order mode, thereby significantly enhancing the excitement of the LSPR to obtain 2.5 times higher RI sensitivity than the U-type [52, 53].
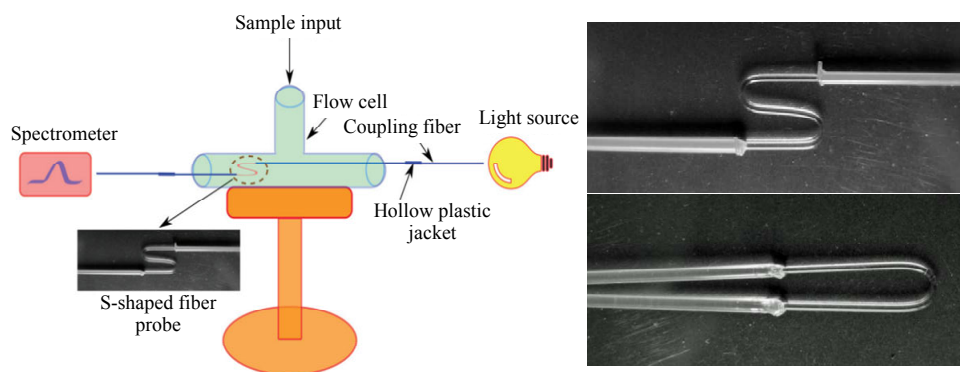

Fig. 5 S-shaped FOLSPR sensor and SEM images of both the S-shaped fiber and U-shaped fiber [49, 50].

The above-mentioned types of fibers involve stretching and bending the fiber into different shapes without altering the fiber structure. In contrast, D-shaped fibers are created by partially removing the cladding or removing both the cladding and a portion of the fiber core to form the structure [54] [Fig. 4(d)]. This structure can expose the more evanescent field and provide a flat detection plane to the analytical environment, thereby inducing a

stronger LSPR signal and offering a stable platform for biomolecular analysis [55]. However, the grinding and polishing of the D-shaped fiber may introduce surface roughness, which causes a potential decrease in the sensitivity. Additionally, conducting tapering treatment on the D-shaped fiber can further enhance the sensitivity, increasing it to over 10 times that of a regular fiber LSPR sensor [56]. Furthermore, the expanded planar sensing area

of the D-shaped fiber enables the creation of periodic nanostructures [57] or the assembly of 3-dimensional (3D) hybrid multilayer structures [58] to facilitate sensitization and multiplexing in the LSPR sensing.

These various types of optical fibers, geometric structures, and transmission schemes mentioned above can be freely combined, and even multiple geometric structures and types can be used together to achieve the higher sensitivity and meet the specific application requirements. In practical applications, we also need to consider factors such as the manufacturing cost and complexity, sensor stability and durability, and transmission distance, and then tailor the design of the LSPR sensing system accordingly.

3. Fabrication technology for the LSPR sensing region

In addition to the geometric parameters of the optical fiber, the performance of the optical fiber LSPR sensor is also influenced by the nanostructure configuration of the sensing region. The nanostructure configuration of the sensing region includes the shape, size, and arrangement of the metal nanoparticles, which play a crucial role in regulating the interaction between the nanoparticles and light, thus impacting the intensity and frequency of the LSPR effect. By optimizing the nanostructure configuration, the sensitivity, selectivity, and stability of the sensor can be adjusted, enabling more accurate and reliable bio-analysis and environmental monitoring. Different application requirements may require different nanostructure configurations. Hence, when designing an optical fiber LSPR sensor, it is crucial to comprehensively consider the relationship between the nanostructure parameters and sensor performance to meet the specific application requirements.

3.1 Self-assembly of nanoparticles

Currently, noble metal nanoparticles, such as AuNPs [59], gold nanorods [60], and silver nanoparticles [61], are commonly used for optical fiber LSPR sensors. Among these, gold-based nanoparticles are particularly advantageous due to their excellent structural stability, oxidation resistance, and biocompatibility. As a result, they are extensively utilized in experimental studies. The predominant approach for immobilizing nanoparticles in the sensing region of the fiber involves chemically bonding the nanoparticles to the modified sensing surface using chemical reagents and functional groups, thus achieving the self-assembly of the sensing structure.

In recent years, there have been numerous reports on the application of self-assembled gold nanoparticle layers in optical fiber LSPR sensing, and these studies primarily rely on two methods. The most commonly employed approach involves hydroxyl silanization on a glass substrate using silane coupling agents. This enables the capture of AuNPs through the amino or thiol terminal groups of the self-assembled film, facilitating the preparation of the sensing region [Fig. 6(a)]. The silane method encompasses two modification schemes: amine silanization and thiol silanization. Amine silanization is based on the principle of positive and negative adsorption effects. It entails the use of solutions like (3-aminopropyl) triethoxysilane [62] (APTES) or (3-aminopropyl) trimethoxysilane [63] (APTMS) to amino-functionalize the surface of the optical fiber through an amination reaction, thus imparting a positive charge. Consequently, the negatively charged nanoparticles can be bound to the positively charged optical fiber surface through electrostatic forces, particularly the interaction of ionic bonds. Thiol silanization, on the other hand, involves functionalizing the sensing region using (3-mercaptopropyl) trimethoxysilane (MPTMS) [60]. The principle of this method is as follows: the methoxy groups (Si-OCH$_3$) of MPTMS can be hydrolyzed into silanol groups (Si-OH). The

interaction between $Si-OCH_3$ and partially hydrolyzed silanol groups results in the formation of a self-assembled film with thiol groups covering the surface of the optical fiber. The AuNPs can then be captured by the thiol groups on the surface, forming covalent Au-S bonds and self-assembling into a monolayer on the optical fiber.

Another commonly used method relies on the electrostatic adsorption effect, utilizing the electrostatic layer-by-layer self-assembly of polyelectrolytes and the surface charge of nanoparticles for the self-assembly of nanostructures

[64] [Fig. 6(b)]. In this approach, negatively charged hydroxylated fiber surfaces asre used to sequentially adsorb multiple layers of polyelectrolytes with opposite charges, followed by the adsorption of charged nanoparticles onto the corresponding polyelectrolyte layers to prepare the sensor. Cationic polyelectrolytes commonly used in this method include poly(allylamine hydrochloride) (PAH) and poly(diallyldimethylammonium chloride) (PDDA), while anionic polyelectrolytes include poly(styrene sulfonate) (PSS) and poly(acrylic acid) (PAA).

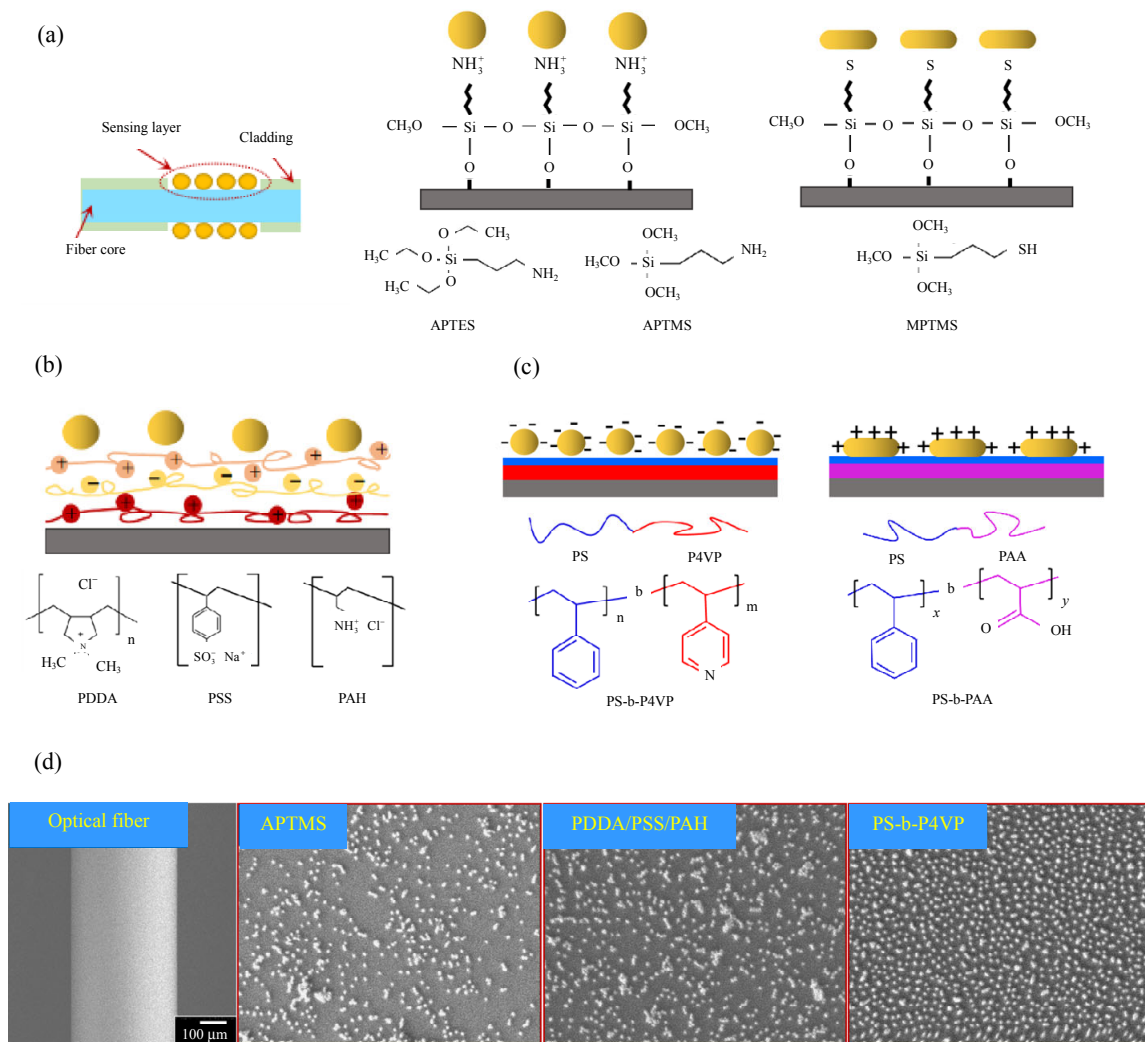The silane coupling method is characterized by a prolonged modification time for the fiber surface

Fig. 6 Nanoparticles-based self-assembly methods for fiber optic LSPR sensor fabrication: (a) silane method by APTMS, APTES or MPTMS, (b) electrostatic layer-by-layer self-assembly method by polyelectrolytes, (c) block copolymer templated method by PS-b-P4VP or PS-b-PAA, and (d) SEM images comparison of silane, electrostatic layer-by-layer, and BCP methods.

and strict control of various conditions, such as temperature. Furthermore, experimental data indicate a relatively low coverage of nanoparticle monolayers obtained through self-assembly, which somewhat restricts its potential for application in the fabrication of high-performance, large-scale, and cost-effective fiber sensors. Conversely, the layer-by-layer self-assembly method employing polyelectrolytes demonstrates a rapid electrostatic adsorption rate, resulting in a substantial reduction in deposition time and operational complexity while enhancing the particle surface coverage. This methodology effectively addresses the limitations of the silane method. Nevertheless, it unavoidably leads to particle aggregation and stacking, consequently diminishing the repeatability and stability of the sensor.

Therefore, in recent years, new methods have been proposed to address the limitations of traditional self-assembly methods, such as the seed-mediated growth method [65]. This method begins by amino-functionalizing the fiber endface using 3-(ethoxydimethylsilyl)-propylamine and then attaching gold nanoseeds onto the amino groups. The particles fixed on the fiber surface are then enlarged through in situ seed-mediated growth to create a sensing surface. This method effectively prevents excessive particle aggregation and ensures uniform distribution. However, it is associated with challenges such as an inconsistent particle diameter and a more complex preparation process.

In 2019, a novel and versatile self-assembly method was proposed for the fabrication of fiber LSPR sensors [66]. This method utilizes a block copolymer-based template to guide the self-assembly of nanoparticles on the template surface, resulting in the high coverage, low aggregation, and controllable nanostructures [Fig. 6(c)]. Block copolymers consist of two chains with distinct properties: a hydrophilic segment and a hydrophobic segment. When dissolved in organic solvents, the hydrophilic segments spontaneously form the outer layer of micelles, while the hydrophobic segments form the inner core through Van der Waals forces and hydrogen bonding. In the presence of a sufficient solvent volume, the block copolymers mainly exist as dispersed individual chains. Thus, by immersing a hydroxylated fiber in an organic solution of block copolymers and employing a simple dip-coating technique, the block copolymer template can be uniformly deposited within seconds. By adjusting parameters such as the polymer solution concentration and block length ratio, it is possible to control the template morphologies and achieve different configurations of self-assembled metal nanoparticles. At high concentrations, the polymer forms highly ordered structures, such as micelles or vesicles, and the metal nanoparticles assemble on the surface as small clusters directed by the polymer. As the solution concentration decreases, the copolymers adhere to the substrate as nanoscale films, facilitating the uniform self-assembly of nanoparticles on the polymer film surface and leading to low aggregation and high coverage monolayer nanostructures. The controllable and precise self-assembly is based on the fact that the multiple hydrogen bonding sites on the hydrophilic segments bind to the hydroxylated substrate, while the metal nanoparticles are bound to the hydrophilic segments through surface charges, such as electrostatic adsorption and ionic bonding. The presence of free hydrophobic polystyrene (PS) chains prevents particle aggregation. This approach results in nanostructures with a desirable surface morphology characterized by the high coverage and low aggregation. It is worth mentioning that it allows for the use of various types and block length ratios of block copolymers for template fabrication. For instance, PS-b-P4VP and PS-b-PAA can be employed to produce ordered templates where P4VP chains bind negatively charged nanoparticles through protonated amino groups, and PAA chains bind positively charged nanoparticles through deprotonated carboxyl groups, respectively [67].

Consequently, this enables effective surface self-assembly of both negatively and positively charged gold nanospheres/nanorods [68]. When compared to the traditional methods mentioned above [Fig. 6(d)], the results demonstrate that gold nanospheres assembled using APTMS or PDDA/PSS/PAH can cover the entire surface but exhibit nonuniform dispersion and aggregation. In contrast, gold nanospheres assembled using PS-b-P4VP can not only achieve the complete surface coverage, but also exhibit uniform dispersion without particle aggregation and form a monolayer nanostructure. In terms of the surface coverage, the PS-b-P4VP method demonstrates the significantly higher performance (18.3±0.3%) compared to the other two methods (12.2±0.4% for APTMS and 15.5±0.8% for PDDA/PSS/PAH). In a word, the block copolymer template method effectively reduces particle aggregation, enhances particle surface coverage, and holds a great potential for improving sensing sensitivity and stability, simplifying the preparation process, and reducing costs.

3.2 Assembly and transfer of periodic array nanostructures

Apart from the conventional chemical self-assembly methods, researchers have also investigated non-chemical bonding strategies for the fabrication of sensing regions. Techniques such as focused ion beam (FIB) milling, micro electro mechanical systems (MEMS), and electron beam lithography (EBL) have been employed to create periodic nanoarrays, which can be effectively utilized in fiber LSPR sensors.
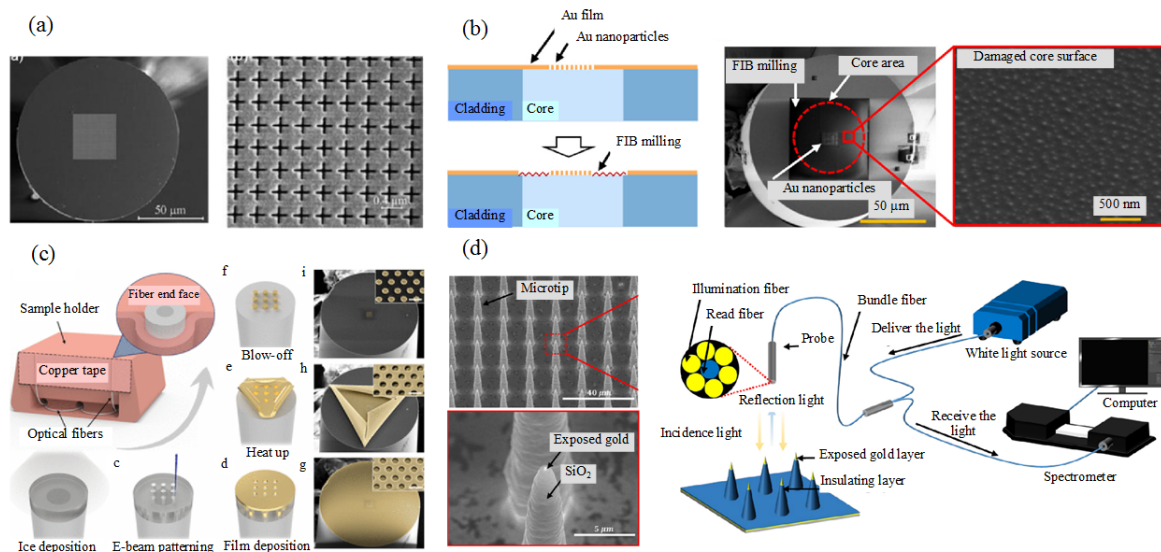

Fig. 7 Non-chemical bonding strategies for the fabrication of sensing regions: (a) cross-shaped nanoarrays [69], (b) AuNPs arrays [70], (c) nanodisk arrays [71], and (d) array of noble metal nanostructures on a silicon microtip [72] on the end face of fibers.

Among these strategies, FIB milling is primarily utilized for the fabrication of periodic nanostructures such as nanoholes, disks, and pillars on the end face of optical fibers. The cross-shaped nanostructure is fabricated on the end face of the fiber, as shown in Fig. 7(a) [69]. H. M. Kim *et al*. [70] successfully employed FIB milling to create AuNPs arrays on the core end face of an optical fiber [Fig. 7(b)], achieving a refractive index sensitivity of 5 700/RIU. Although FIB milling enables the production of uniformly structured nanoarrays with stable sensing performance, its low success rate, high cost, and complex manufacturing process limit its suitability for large-scale processing applications. In Fig. 7(c), Y. Hong *et al*. [71] proposed a solvent-free nanofabrication method based on the emerging

ice-assisted electron beam lithography (iEBL) technique, which offers a streamlined and eco-friendly approach for implementing e-beam patterning on substrates with arbitrary shapes. They successfully fabricated periodic nanostructures, including silver concentric rings, V-shape nanoantenna arrays, bowtie arrays, and ring arrays. This method allows for the production of diverse and highly uniform structures, and offers a lower cost and higher success rate compared to FIB milling. However, the fabrication process remains relatively complex. The MEMS technique was also employed to fabricate a uniformly distributed array of noble metal nanostructures on a silicon microtip on the end face of an optical fiber [72], as shown in Fig. 7(d). The resulting LSPR sensor demonstrated the excellent reproducibility, stable reliability, and favorable optical properties in the measurement system. The periodic and long-lasting particle array achieved through the MEMS technology positions it as a promising method for commercialized LSPR applications.

In conclusion, both self-assembly and periodic array assembly methods have their own advantages and disadvantages. The self-assembly method is characterized by the simple preparation process and lower cost. However, it is challenging to precisely control the self-assembly of nanoparticles during the binding process, resulting in the distribution of particles in a dispersed and disordered structure. Furthermore, issues such as local particle shedding and aggregation can have an impact on the performance of the sensor. On the other hand, the periodic array assembly method enables the creation of highly ordered periodic nanoarrays, leading to sensors with the high sensitivity, repeatability, and stability. However, this method requires the utilization of advanced micro/nano fabrication techniques, which significantly elevates the manufacturing costs. Additionally, the substrates used in this method are mostly flat, which restricts the fabrication of structures to D-type or

fiber endfaces, thereby presenting implementation challenges.

4. Applications of the FOLSPR biosensor

The FOLSPR sensor has emerged as a promising tool for biosensing applications. It offers several advantages over other sensing configurations. The LSPR is a phenomenon occurring when noble metal nanoparticles are excited by light, resulting in strong absorption and scattering at specific wavelengths. By immobilizing biomolecules on the surface of these nanoparticles, changes in the local RI caused by biomolecular interactions can be detected. The unique properties of the FOLSPR sensor make it suitable for various biological detection scenarios. The small size and flexibility of optical fibers enable easy integration into complex biological systems, such as implantable devices or lab-on-a-chip platforms. This allows for real-time, remote, and minimally invasive monitoring of biomolecular interactions. Moreover, the localized nature of the LSPR in nanoscale regions ensures the high sensitivity and label-free detection. This eliminates the need for bulky labels or tags, making it a suitable technique for multiplexed assays and high-throughput screening. Furthermore, the tailored design and fabrication of metal nanoparticles or nanoarrays can enhance the sensitivity and selectivity of the sensor for specific target molecules. The versatility of fiber optic LSPR sensors allows for the detection of a wide range of analytes, including proteins, pathogens and cells, nucleic acids (DNA and RNA), and other small biomolecules (organic compounds and heavy metal ions).

Protein immunoassay is currently the most widely studied application of FOLSPR biosensors. The general protein molecular detection and signal amplification strategies are shown in Fig. 8. Typically, the sensing region of the nanoparticles/periodic structure surface is modified by thiol through the gold sulfur bond with a carboxyl
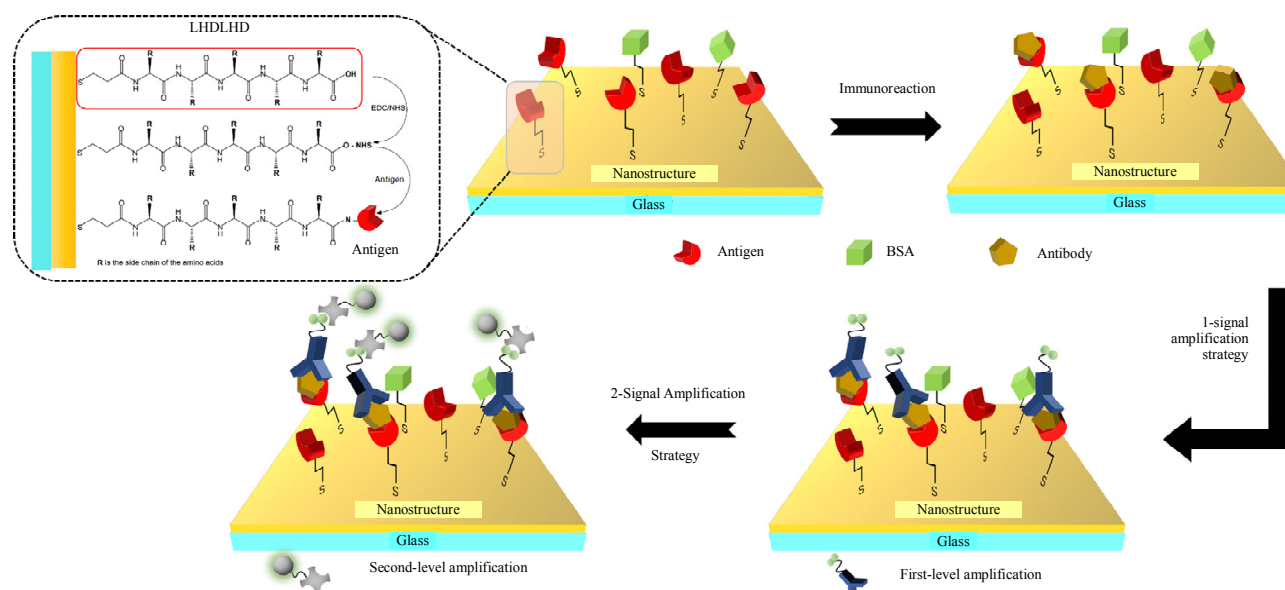
Fig. 8 Schematic diagram of the typical antigen-antibody immunoassay sensing process.

group at the other end. An antibody or antibody fragment is immobilized as a biorecognition element on the monolayer through the carboxyl group, which has been pre-activated using the EDC/NHS [1-ethyl-3-(3-dimethylaminopropyl) carbodiimide hydrochloride (EDC), N-hydroxysuccinimide (NHS)] solution. When the corresponding antigen is bound to the surface- immobilized antibody within the electric field range, this interaction disrupts the plasmon and results in a change in the reflection intensity, allowing for the determination of the analyte concentration. Of course, in addition to thiol, other reagents such as peptides and dextran are also modified on the sensing region surface to generate more anchoring points. Due to the large differences in the molecular weight of various proteins, the local field changes induced by the binding of target proteins with capture probes also vary, leading to different detection sensitivities. For large proteins, such as IgG, their high mass is sufficient for sensitive sensing and can be directly monitored [66, 73]. Conversely, a small molecule immunoassay application is challenging. The small size of the target protein itself is unable to generate a sufficient LSPR signal, the antibody-antigen binding induces

only a small mass variation, which cannot provide sensitive analysis. Therefore, amplification strategies, such as sandwich assays [64, 74], are required to enhance the signal [37]. H. M. Kim *et al*. [74] reported a sandwich assay for ultrasensitive thyroglobulin (Tg) detection by implementing a second antibody and a second gold nanoparticle signal amplifier, as shown in Fig. 9. The limit of detection (LOD) is improved by approximately 15 times from 97.6 fg/mL to 6.6 fg/mL.

Nucleic acids serve as a reservoir of genetic information in the human body, and their polymorphism analysis and mutation detection can effectively diagnose conditions like tumors and infectious diseases. Typically, the double-stranded structure of the deoxyribonucleic acid (DNA) is disrupted by high temperature or high pH, and the sequence is determined through hybridization with single-stranded DNA (ssDNA) fragments. However, enzymatic or fluorescent labeling detection methods are time-consuming and may interfere with molecular interactions by obstructing active binding sites, resulting in unreliable detection results. Consequently, the FOLSPR has been introduced as a portable and highly sensitive sensor for the
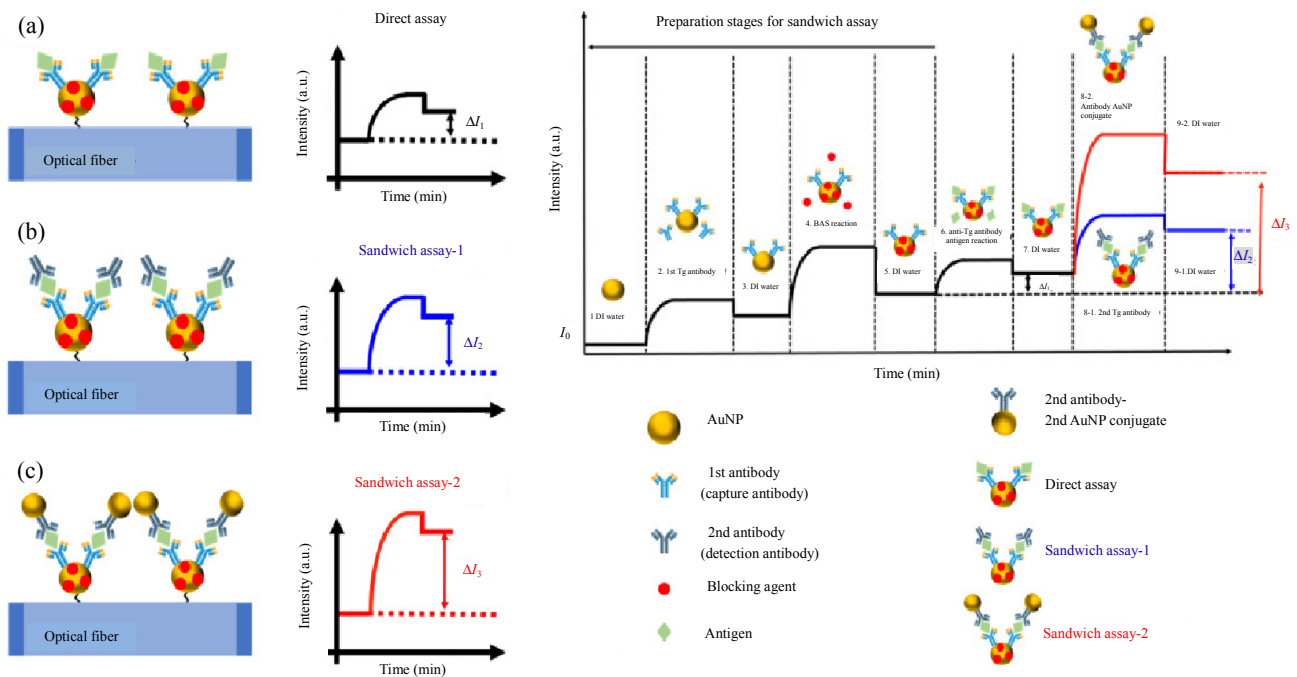
Fig. 9 Schematic diagram of thyroglobulin by the direct antibody, secondary antibody sandwich assay, and antibody-gold nanoparticle conjugate sandwich assay [74].

label-free detection of ssDNA, yielding promising results. In this technique, the captured ssDNA is immobilized on the sensor surface via gold-sulfur bonds. If the corresponding complementary target ssDNA is present in the sample, it will hybridize with capture ssDNA [75]. This binding event on the nanoparticles disturbs localized surface plasmons, altering the resonance conditions and causing changes in optical signals. However, if the quantity of target ssDNA is insufficient to induce the LSPR, a sandwich structure is employed to enhance the detection signal. As shown in Fig. 10, the capture ssDNA only hybridizes with one half of the target ssDNA, while the other half of the target ssDNA is then hybridized with another probe ssDNA. The probe ssDNA is pre-modified with signal amplification molecules on one end to achieve the secondary signal amplification. The signal amplification molecules can be fluorescent dyes, proteins, AuNPs, or other substances, depending on the specific requirements of spectroscopy, imaging,

and other detection methods [68, 76–78]. Moreover, some reported nucleic acid detection strategies (Fig. 11) used for SPR sensors are also applicable to fiber LSPR sensors, including competitive detection of micro ribose nucleic acid (miRNA), sandwich-based detection of ssDNA, and aptamer-based detection, among others [79–82]. As shown in Fig. 11(a), in the presence of target cfDNA, the hairpins H_1-AuNPs and H_2 are triggered by the hybridization chain reaction (HCR), and then the Ω-shaped FOLSPR biosensor fabricated with the capture DNA captures the HCR product for synergistically amplified the LSPR signal [79]. S. Y. Qian *et al.* [82] proposed a phenylboronic acid (PBA) probe for miRNA detection, as shown in Fig. 11(b), both the target miRNA and subsequently complementary ssDNA were hybridized with capture ssDNA. The PBA-AuNPs could further bind with ribose in miRNA (two hydroxyl groups) rather than deoxyribose in complementary ssDNA to amplify the sensing signal.
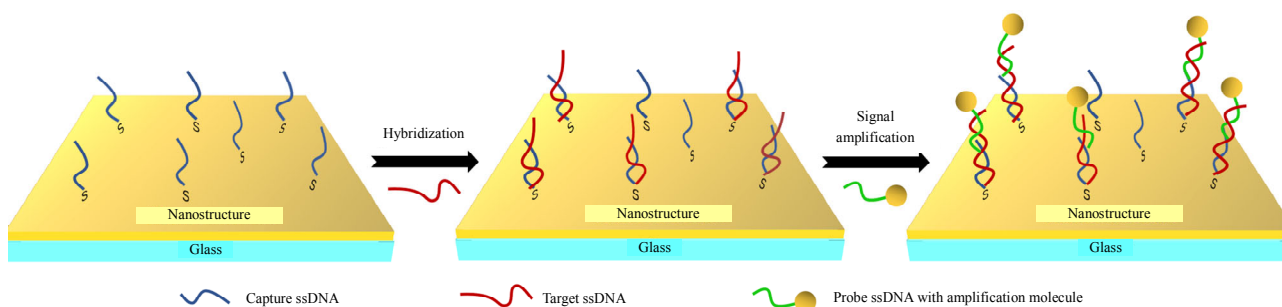
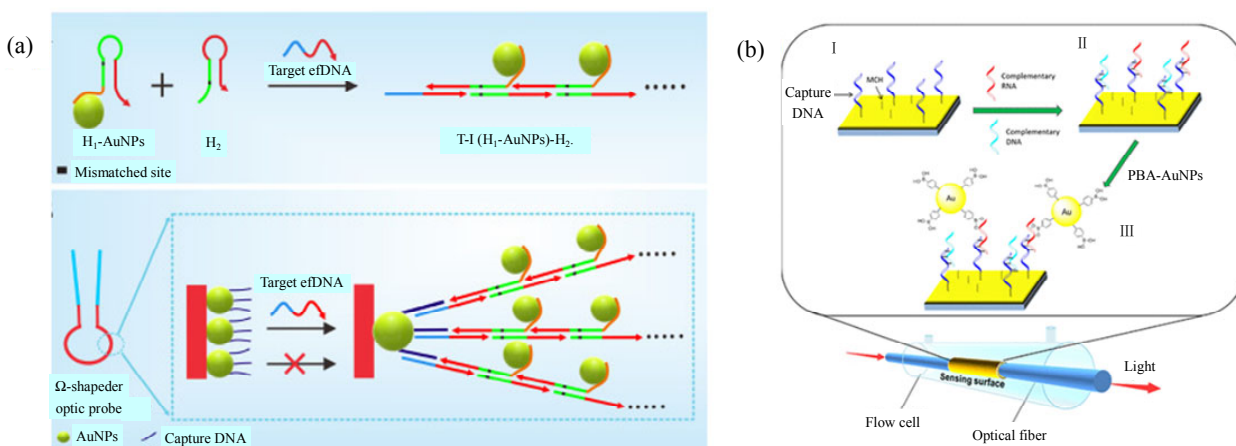Fig. 10 Schematic diagram of the ssDNA sensing detection process.

Fig. 11 Schematic diagram of signal amplification strategies for nucleic acid detection: (a) multistage nanoparticle amplification [79] and (b) boric acid-gold nanoparticle sandwich assay [82].

In addition, detection strategies for other molecules are similar to those for proteins and nucleic acids as mentioned above. The detection strategy can be determined based on the size of the target molecule. In particular, for the detection of microorganisms such as living cells, bacteria, and viruses can be used to directly capture them onto the surface of the fiber sensor for detection. Z. Luo *et al.* [83] developed a U-shaped FOLSPR biosensor for the colorectal cancer cell detection. As shown in Fig. 12(a), the cell could be captured by immobilizing Con A onto the fiber through specific binding between Con A and the N-glycan expression on the cell surface. The cytosensor affords the ultrasensitivity for the cancer cell detection with the LOD of 30 cells/mL and good linearity in a wide range of 1×10^2 cells/mL–1×10^6 cells/mL. Furthermore, the FOLSPR biosensor can also be

employed to inactivate tumor cells by in-site laser heating or other photothermal therapies, thus achieving therapeutic purposes [53]. The Ω-shaped FOLSPR biosensor [Fig. 12(b)] is also designed for the real-time and label-free bacterial detection [84]. The surface-immobilized aptamers specifically capture the salmonella typhimurium, resulting in the LOD down to 128 CFU/mL within a linear range from 5×10^2 CFU/mL to 1×10^8 CFU/mL, which demonstrates a better selectivity for the salmonella typhimurium detection compared to other bacteria. S. Kumar *et al*. [85] proposed an LSPR biosensor, which used an MCF with seven cores arranged in a hexagonal pattern, was spliced with the SMF for the shigella bacteria detection, and displayed a wide linear detection range from 1 CFU/mL to 10^9 CFU/mL with a low LOD of 1.56 CFU/mL. As shown in Fig. 12(c), the etching process increases

evanescent waves and mode coupling between MCF cores, while the coating with AuNPs and molybdenum disulfide enhances the excitation of localized plasmons. The J-shaped optical fiber is obtained by folding an Ω shape, and as shown in Fig. 12(d), a spacer nucleic acid with the short stem-loop structure is adopted to control the aptamer density and further enhance the LSPR signal response [86]. This proposed biosensor could realize label-free and sensitive detection of helicobacter

pylori in 30 min with an LOD as low as 45 CFU/ml and a wide linear range from 1×10^2 CFU/mL to 1×10^8 CFU/mL. In general, for the detection of cells or bacteria, the detection schemes are typically label-free, using aptamers to specifically capture the target bacteria or cells. Additional enhancement molecules, such as molybdenum disulfides or nucleic acids, can further improve the LOD and achieve ultra-trace identification.
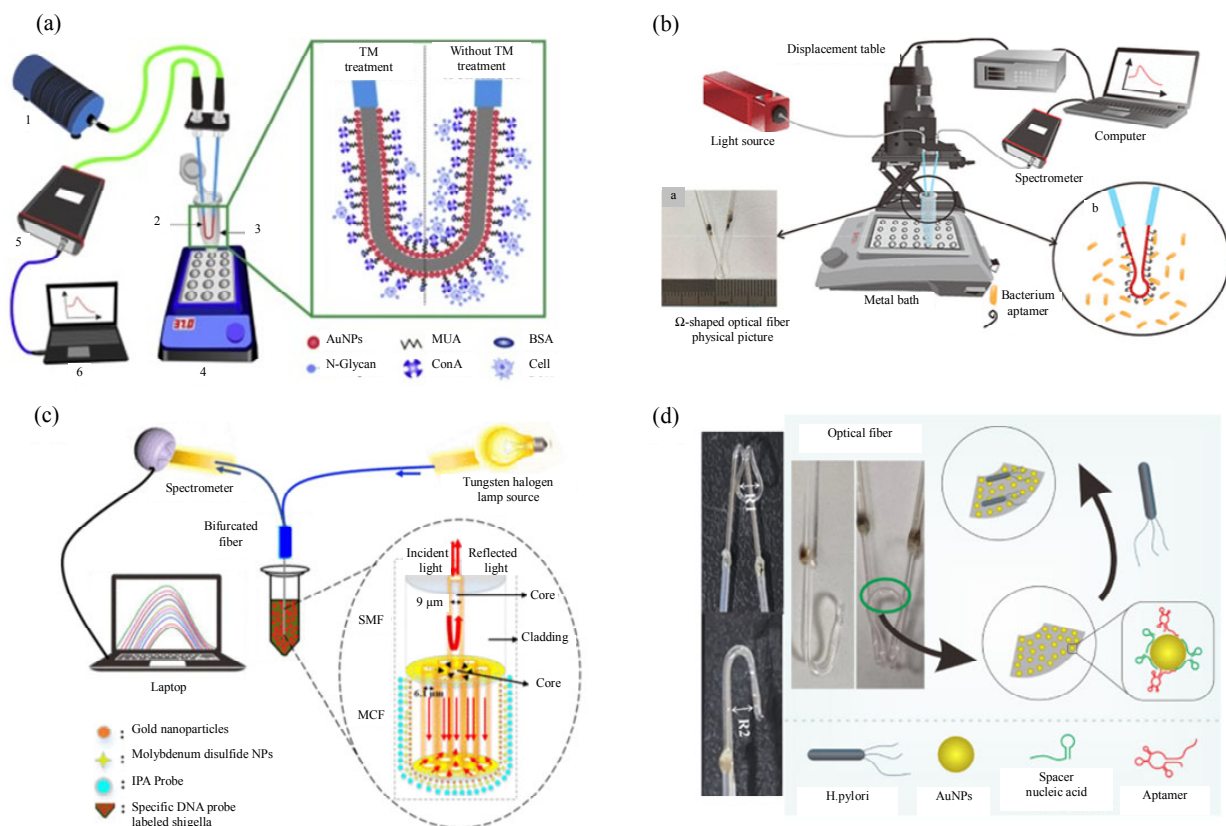
Fig. 12 Schematic diagram of FOLSPR biosensors for the microorganisms detection: (a) U-shaped FOLSPR biosensor for the cancer cell detection [83], (b) Ω-shaped FOLSPR biosensor for the salmonella typhimurium detection [84], (c) MCF-SMF FOLSPR biosensor for the shigella bacteria detection [85], and (d) J-shaped FOLSPR biosensor for the helicobacter pylori detection [86].

For small molecules, such as the cholesterol, ascorbic acid, creatinine, and glucose, specific capture probes can be directly immobilized on the surface of the fiber to achieve the detection by the specific binding between the capture probe and the target molecule. Commonly used capture probe molecules in this case include the boronic acid,

streptavidin, and enzymes. Enzymes, in particular, exhibit high catalytic specificity in certain chemical reactions. By selecting the appropriate enzyme as the recognition element for the target molecule, the higher specificity and selectivity can be achieved. Glucose oxidase is an enzyme that catalyzes the oxidation of glucose. By immobilizing glucose

oxidase on the surface of a U-shaped FOLSPR sensor, blood glucose levels can be measured rapidly in a very short period of time [87]. This method requires only about 150 μL of the blood sample. On the other hand, for smaller molecules such as the heavy metal ions, secondary signal amplification strategies are required to detect molecular interactions at ultra-low concentrations. Similar to nucleic acid detection structures, sandwich assays, nanomaterial enhancement approaches, and other techniques can be utilized to achieve the detection of molecular interactions at extremely low concentrations. S. Jia *et al.* [88] presented a wavelength-modulated FOLSPR sensor coated by gold nanospheres for the highly sensitive Hg^{2+} detection (LOD: low to 0.7 nM) based on

thymine-Hg^{2+}-thymine base pair mismatches system, as shown in Fig. 13(a). Zearalenone (ZEN), a toxin produced when crops are moldy, enables the portable and rapid trace detection using FOSPR biosensors. The ZEN nucleic acid aptamer is modified on the cross-section of the end of the FOSPR sensor for the ZEN detection [Fig. 13(b)] with a low LOD of 0.102 ng/mL. We also summarize some typical FOLSPR biosensors in Table 1, including their targets, fiber structures, detection formats, and performances.

It is noteworthy that in addition to employing the direct detection and multistage enhancement strategies, researchers have also experimented with the use of two-dimensional nanomaterials to enhance the sensitivity of FOLSPR sensors. Among
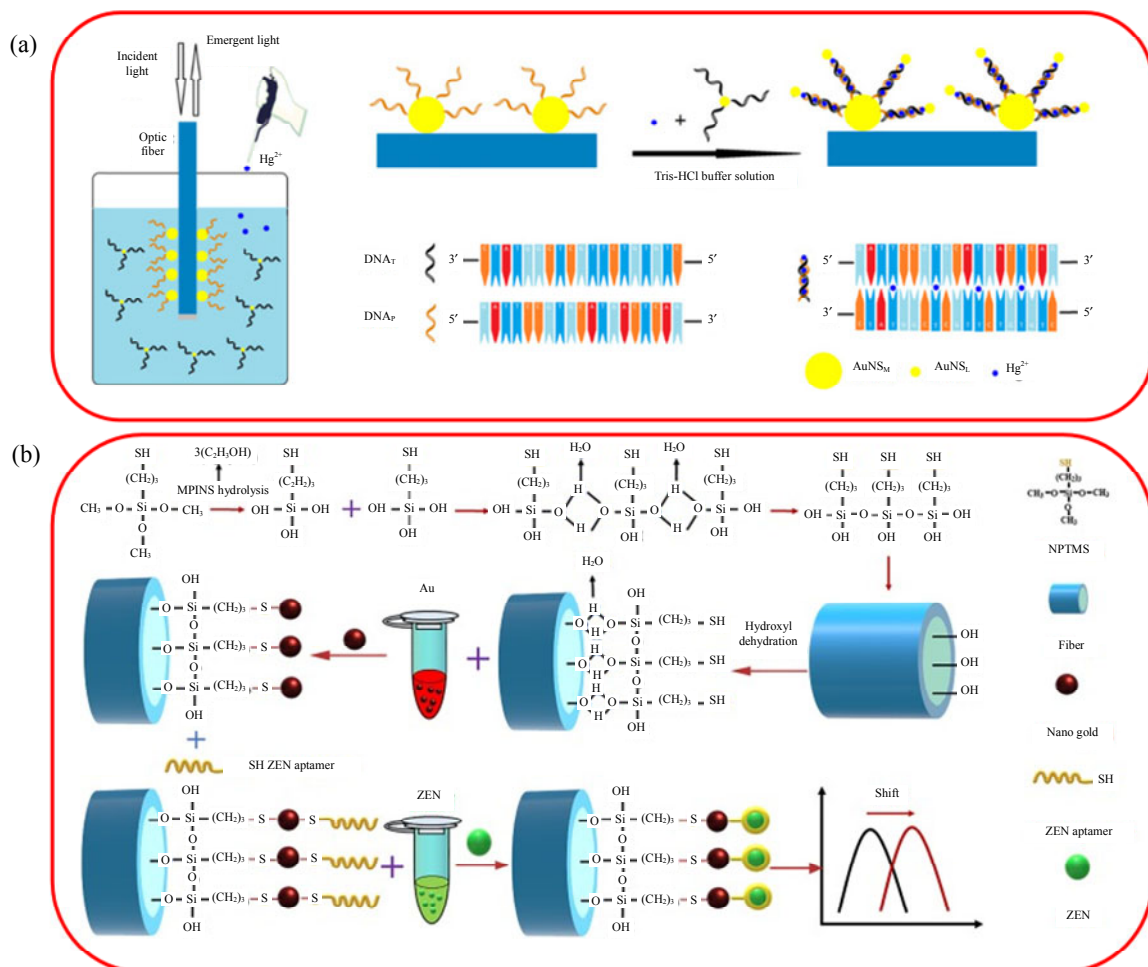

Fig. 13 Schematic diagram of FOLSPR biosensors for small molecules including (a) heavy metal ion Hg^{2+} [88] and (b) food toxin ZEN [89].

them, the graphene oxide (GO) has received the most widespread attention. The emerging GO has been widely introduced into FOLSPR biosensing due to its abundant oxygen functional groups and large specific surface area, which effectively enhances the functionalization of biomolecules and improves the sensing performance of bio-molecules. B. B. Luo *et al*. [90] achieved a highly tilted fiber gratings (ExTFG) LSPR sensor by decorating gold nanoshells on the surface of ExTFG and then depositing functionalized GO on the sensor surface to identify sPD-L1 monoclonal antibodies in the human serum of liver cancer patients. The sensor exhibits a detection range for sPD-L1 of 0.04 pM–4 pM with an LOD of 0.04 pM. In addition, an FOLSPR sensor can also be prepared by growing AuNPs in situ on GO and subsequently coating the composite material onto the fiber surface [16]. This sensor is employed for the detection of T-2 toxin in food, demonstrating an LOD of 0.249 ng/mL. Moreover, it exhibits the remarkable resistance to interference from other toxins, including zearalenone, aflatoxin B_1, vomitoxin, and ochratoxin A.

Table 1 Recognition methods, target molecules and performances of different specialty fiber optic LSPR biosensors.

Target	Technique	Detection format	Performance	Ref.
Human IgG	Straight MMF	Direct	LOD: 0.8 nM	[66]
AFP	U-bend MMF	Direct	LOD: 0.85 ng/mL	[91]
Transferrin	HCF	Direct	Range: 0.01 mg/mL–0.15 mg/mL	[19]
Thyroglobulin	Straight MMF	Direct	LOD: 0.19 pg/mL	[92]
f-PSA	SMF	Direct	LOD: 100 fg/mL	[93]
Cardiac troponin I	MMF-photosensitive-MMF	Sandwich	LOD: 96 ng/mL	[37]
rop B ssDNA	Straight MMF	Sandwich	LOD: 67 pM	[80]
cfDNA	Ω-type MMF	HCR-AuNPs	LOD: 14.0 pM	[79]
MCF-7 cancer cells	Ω-type MMF	Direct	LOD: 12 cells/mL	[51]
E.coli B40	U-bend MMF	Phage T4	Detection range: 10^2 CFU/mL–10^7 CFU/mL	[94]
Shigella bacteria	SMF-PCF	MoS$_2$-DNA	LOD: 1.56 CFU/mL	[85]
Salmonella typhimurium	Ω-type MMF	Sandwich	LOD: 108.4 CFU/mL (10 min) 7.4 CFU/mL (100 min)	[52]
Cholesterol	SMF-HCF	enzyme	LOD: 25.5 μM	[95]
Ascorbic acid	SMF-photosensitive	enzyme	LOD: 15.12 μM	[96]
Creatinine	SMF-MCF-MMF-SMF	enzyme	LOD: 128.4 μM	[97]
Glucose	Tapered SMF	Direct	LOD: 1.06 nm/mM	[98]
ALT enzyme	Tapered-in-taper SMF	Sandwich	Sensitivity: 4.1 pm/(U/L)	[43]
Hg^{2+}	Straight MMF	ssDNA mismatch	LOD: 0.7 nM	[88]
Zearalenone	Straight MMF	Aptamer	LOD: 0.102 ng/mL	[89]

5. Conclusions and outlook

In summary, the fiber optic LSPR based on the well-ordered nanoparticles monolayer or periodic nanostructures under certain conditions leads to the greater enhancements of localized electric fields compared to the SPR without the nanomaterials and also provides the appropriate solution for the micro-smart biological integrated sensor. To enhance the sensing performance of FOLSPR sensors, various techniques can be used, such as using different types of fibers with optimized geometric structures (the types of fibers include SMF, MMF, PCF, HCF, and FBG, and the shapes include tapered,

U-type, Ω-type, and D-type), as well as utilizing advanced surface assembly schemes to achieve ordered monolayers of nanoparticles or periodic nanostructures to enhance the sensitivity and stability of sensors, and customizing recognition and quantitative analysis strategies can be tailored to specific biomolecules. In the field of biomedical diagnostics, they can be used for the label-free detection of biomarkers, DNA hybridization, protein-protein interactions, and pharmaceutical analysis. Moreover, the ongoing development of the compact, portable, and cost-effective instrumentation is expected to facilitate the widespread adoption of these biosensors in various fields. Hence, FOLSPR biosensors are poised to revolutionize the field of biosensing, enabling the rapid and accurate biomolecules detection, disease diagnosis, and environment monitoring in real time.

While FOLSPR biosensors have found extensive structures, manufactures, and bio-applications, there is still ongoing research to further enhance their performance. As a result, there are several areas where the development of FOLSPR biosensors is anticipated.

(1) Development and application of the multi-channel FOLSPR biosensors

Currently, most bio-applications require quantitative detection of multiple biomolecules or elimination of interferences from unrelated molecules. In order to reduce the complexity and cost of measurement systems and enable simultaneous assessment of multiple parameters related to diseases or the environment, the design of FOLSPR biosensors that can simultaneously measure multiple biomolecules or perform multiple measurements of the same biomolecule in a multi-channel FOLSPR biosensor will be an effective development approach in practical applications.

(2) Utilization of new materials and technological innovations for enhancing the sensitivity of FOLSPR biosensors

We mention the promising advancements in improving the sensitivity of FOLSPR biosensors using two-dimensional materials, such as molybdenum disulfide and graphene oxide. By incorporating advanced materials, such as carbon nanotubes, it is possible to enhance the contact area between the sensing surface and target molecules through the optimized design of the sensing layer structure. Additionally, by manipulating the parameters of the sensitizing layer of two-dimensional materials, such as the tunable band gap and excellent electronic transport properties of black phosphorus, the local electromagnetic field effect on the sensing surface can be intensified. These approaches have the potential for offering new possibilities for further enhancing the sensing performance.

Acknowledgment

Declarations

References

[1]   J. M. Pitarke, V. M. Silkin, E. V. Chulkov, and P. M.

Echenique, "Theory of surface plasmons and surface-plasmon polaritons," *Reports on Progress in Physics*, 2006, 70(1): 1–87.

[2] A. V. Zayats, I. I. Smolyaninov, and A. A. Maradudin, "Nano-optics of surface plasmon polaritons," *Physics Reports*, 2005, 408(3–4): 131–314.

[3] J. Homola, S. S. Yee, and G. Gauglitz, "Surface plasmon resonance sensors: review," *Sensors and Actuators B*: *Chemical*, 1999, 54(1–2): 3–15.

[4] J. Homola, "Surface plasmon resonance sensors for detection of chemical and biological species," *Chemical Reviews*, 2008, 108(2): 462–493.

[5] M. D. Lu, Y. Z. Liang, S. Y. Qian, L. X. Li, Z. G. Jing, J. F. Masson, *et al*., "Optimization of surface plasmon resonance biosensor with Ag/Au multilayer structure and fiber-optic miniaturization," *Plasmonics*, 2017, 12(3): 663–673.

[6] E. Hutter and J. H. Fendler, "Exploitation of localized surface plasmon resonance," *Advanced Materials*, 2004, 16(19): 1685–1706.

[7] J. N. Anker, W. P. Hall, O. Lyandres, N. C. Shah, J. Zhao, and R. P. Van Duyne, "Biosensing with plasmonic nanosensors," *Nature Materials*, 2008, 7(6): 442–453.

[8] J. Zhao, X. Zhang, C. R. Yonzon, A. J. Haes, and R. P. Van Duyne, "Localized surface plasmon resonance biosensors," *Nanomedicine*, 2006, 1(2): 219–228.

[9] B. Sepúlveda, A. Calle, L. M. Lechuga, and G. Armelles, "Highly sensitive detection of biomolecules with the magneto-optic surface-plasmon-resonance sensor," *Optics Letters*, 2006, 31(8): 1085–1087.

[10] L. K. Chau, Y. F. Lin, S. F. Cheng, and T. J. Lin, "Fiber-optic chemical and biochemical probes based on localized surface plasmon resonance," *Sensors and Actuators B*: *Chemical*, 2006, 113(1): 100–105.

[11] G. Barbillon, J. L. Bijeon, J. Plain, M. L. de la Chapelle, P. M. Adam, and P. Royer, "Electron beam lithography designed chemical nanosensors based on localized surface plasmon resonance," *Surface Science*, 2007, 601(21): 5057–5061.

[12] J. Y. Guang, M. D. Lu, Y. Liu, R. Z. Fan, C. Wang, R. Liu, *et al*., "Flexible and speedy preparation of large-scale polystyrene monolayer through hemispherical-depression-assisted self-assembling and vertical lifting," *ACS Applied Polymer Materials*, 2023, 5(4): 2674–2683.

[13] H. H. Jeong, N. Erdene, S. K. Lee, D. H. Jeong, and J. H. Park, "Fabrication of fiber-optic localized surface plasmon resonance sensor and its application to detect antibody-antigen reaction of interferon-gamma," *Optical Engineering*, 2011, 50(12): 124405.

[14] P. Vaiano, B. Carotenuto, M. Pisco, A. Ricciardi, G. Quero, M. Consales, *et al*., "Lab on fiber technology for biological sensing applications," *Laser & Photonics Reviews*, 2016, 10(6): 922–961.

[15] D. Paul, S. Dutta, D. Saha, and R. Biswas, "LSPR based ultra-sensitive low cost U-bent optical fiber for volatile liquid sensing," *Sensors and Actuators B*: *Chemical*, 2017, 250: 198–207.

[16] Y. C. Xu, M. Xiong, and H. Yan, "A portable optical fiber biosensor for the detection of zearalenone based on the localized surface plasmon resonance," *Sensors and Actuators B: Chemical*, 2021, 336: 129752.

[17] R. C. Jorgenson and S. S. Yee, "A fiber-optic chemical sensor based on surface plasmon resonance," *Sensors and Actuators B: Chemical*, 1993, 12(3): 213–220.

[18] S. M. Chen, Y. Liu, Q. X. Yu, and W. Peng, "Microcapillary-based integrated LSPR device for refractive index detection and biosensing," *Journal of Lightwave Technology*, 2020, 38(8): 2485–2492.

[19] Y. Liu, N. Zhang, P. Li, L. Yu, S. M. Chen, Y. Zhang, *et al*., "Low-cost localized surface plasmon resonance biosensing platform with a response enhancement for protein detection," *Nanomaterials*, 2019, 9(7): 1019.

[20] J. Zhang, J. Yuan, Y. Qu, S. Qiu, C. Mei, X. Zhou, *et al*., "Graphene coated micro-channel fiber sensor based on localized surface plasmon resonance," *Journal of the Optical Society of America B – Optical Physics*, 2023, 40(4): 695–704.

[21] B. T. Wang and Q. Wang, "Sensitivity-enhanced optical fiber biosensor based on coupling effect between SPR and LSPR," *IEEE Sensors Journal*, 2018, 18(20): 8303–8310.

[22] M. A. Mollah and M. S. Islam, "Novel single hole exposed-suspended core localized surface plasmon resonance sensor," *IEEE Sensors Journal*, 2021, 21(3): 2813–2820.

[23] M. S. Islam, M. R. Islam, J. Sultana, A. Dinovitser, B. W. H. Ng, and D. Abbott, "Exposed-core localized surface plasmon resonance biosensor," *Journal of the Optical Society of America B – Optical Physics*, 2019. 36(8): 2306–2311.

[24] R. Singh and S. Dewra, "Performance analysis of localized surface plasmon resonance sensor with and without Bragg grating," *Journal of Optical Communications*, 2019, 41(1): 45–50.

[25] B. R. Heidemann, J. D. Pereira, I. Chiamenti, M. M. Oliveira, M. Muller, and J. L. Fabris, "Matching long-period grating modes and localized plasmon resonances: effect on the sensitivity of the grating to the surrounding refractive index," *Applied Optics*, 2016, 55(32): 8979–8985.

[26] J. X. Zhang, T. M. Liang, H. Y. Wang, Z. L. Huang, Z. J. Hu, K. Xie, *et al*., "Ultrasensitive glucose biosensor using micro-nano interface of tilted fiber grating coupled with biofunctionalized Au nanoparticles," *IEEE Sensors Journal*, 2022, 22(5): 4122–4134.

[27] S. Lepinay, A. Staff, A. Ianoul, and J. Albert,

"Improved detection limits of protein optical fiber biosensors coated with gold nanoparticles," *Biosensors & Bioelectronics*, 2014, 52: 337–344.

[28] B. B. Luo, Y. J. Wang, H. F. Lu, S. X. Wu, Y. M. Lu, S. H. Shi, *et al.*, "Label-free and specific detection of soluble programmed death ligand-1 using a localized surface plasmon resonance biosensor based on excessively tilted fiber gratings," *Biomedical Optics Express*, 2019, 10(10): 5136–5148.

[29] L. Zhang, J. Lou, and L. Tong, "Micro/nanofiber optical sensors," *Photonic Sensors*, 2011, 1(1): 31–42.

[30] K. Li, W. Zhou, and S. Zeng, "Optical micro/nanofiber-based localized surface plasmon resonance biosensors: fiber diameter dependence," *Sensors*, 2018, 18(10): 3295.

[31] P. Uebel, S. T. Bauerschmidt, M. A. Schmidt, and P. S. Russell, "A gold-nanotip optical fiber for plasmon-enhanced near-field detection," *Applied Physics Letters*, 2013, 103(2): 021101.

[32] L. Singh, R. Singh, B. Y. Zhang, B. K. Kaushik, and S. Kumar, "Localized surface plasmon resonance based hetero-core optical fiber sensor structure for the detection of L-cysteine," *IEEE Transactions on Nanotechnology*, 2020, 19: 201–208.

[33] Z. Q. Tou, C. C. Chan, W. C. Wong, and L. H. Chen, "Fiber optic refractometer based on cladding excitation of localized surface plasmon resonance," *IEEE Photonics Technology Letters*, 2013, 25(6): 556–559.

[34] A. Candiani, A. Bertucci, S. Giannetti, M. Konstantaki, A. Manicardi, S. Pissadakis, *et al.*, "Label-free DNA biosensor based on a peptide nucleic acid-functionalized microstructured optical fiber-Bragg grating," *Journal of Biomedical Optics*, 2013, 18(5): 057004.

[35] M. Y. Li, R. Singh, M. S. Soares, C. Marques, B. Y. Zhang, and S. Kumar, "Convex fiber-tapered seven core fiber-convex fiber (CTC) structure-based biosensor for creatinine detection in aquaculture," *Optics Express*, 2022, 30(8): 13898–13914.

[36] B. T. Wang and Q. Wang, "Sensitivity-enhanced optical fiber biosensor based on coupling effect between SPR and LSPR," *IEEE Sensors Journal*, 2018, 18(20): 8303–8310.

[37] Y. Wang, R. Singh, S. Chaudhary, B. Y. Zhang, and S. Kumar, "2-D nanomaterials assisted LSPR MPM optical fiber sensor probe for cardiac troponin I detection," *IEEE Transactions on Instrumentation and Measurement*, 2022, 71: 9504609.

[38] R. Singh, S. Kumar, F. Z. Liu, C. Shuang, B. Y. Zhang, R. Jha, *et al.*, "Etched multicore fiber sensor using copper oxide and gold nanoparticles decorated graphene oxide structure for cancer cells detection," *Biosensors & Bioelectronics*, 2020, 168: 112557.

[39] V. Semwal and B. D. Gupta, "Experimental studies on the sensitivity of the propagating and localized

surface plasmon resonance-based tapered fiber optic refractive index sensors," *Applied Optics*, 2019, 58(15): 4149–4156.

[40] J. Z. Wang, Z. Q. Luo, M. Zhou, C. C. Ye, H. Y. Fu, Z. P. Cai, *et al.*, "Evanescent-light deposition of graphene onto tapered fibers for passive Q-switch and mode-locker," *IEEE Photonics Journal*, 2012, 4(5): 1295–1305.

[41] S. Musolino, E. P. Schartner, G. Tsiminis, A. Salem, T. M. Monro, and M. R. Hutchinson, "A portable optical fiber probe for in vivo brain temperature measurements," *SPIE Biophotonics Australasia*, 2016, 10013: UNSP 100130Q.

[42] S. Ko, J. Lee, J. Koo, B. S. Joo, M. Gu, and J. H. Lee, "Chemical wet etching of an optical fiber using a hydrogen fluoride-free solution for a saturable absorber based on the evanescent field interaction," *Journal of Lightwave Technology*, 2016, 34(16): 3776–3784.

[43] Z. Wang, R. Singh, C. Marques, R. Jha, B. Y. Zhang, and S. Kumar, "Taper-in-taper fiber structure-based LSPR sensor for alanine aminotransferase detection," *Optics Express*, 2021, 29(26): 43793–43810.

[44] J. M. Ward, A. Maimaiti, V. H. Le, and S. N. Chormaic, "Contributed review: optical micro- and nanofiber pulling rig," *Review of Scientific Instruments*, 2014, 85(11): 111501.

[45] G. Zhu, N. Agrawal, R. Singh, S. Kumar, B. Zhang, C. Saha, *et al.*, "A novel periodically tapered structure-based gold nanoparticles and graphene oxide – immobilized optical fiber sensor to detect ascorbic acid," *Optics & Laser Technology*, 2020, 127: 106156.

[46] W. Zhang, R. Singh, Z. Wang, G. R. Li, Y. Y. Xie, R. Jha, *et al.*, "Humanoid shaped optical fiber plasmon biosensor functionalized with graphene oxide/multi-walled carbon nanotubes for histamine detection," *Optics Express*, 2023, 31(7): 11788–11803.

[47] G. R. Li, Q. Xu, R. Singh, W. Zhang, C. Marques, Y. Y. Xie, *et al.*, "Graphene oxide/multiwalled carbon nanotubes assisted serial quadruple tapered structure-based LSPR sensor for glucose detection," *IEEE Sensors Journal*, 2022, 22(17): 16904–16911.

[48] V. V. R. Sai, T. Kundu, and S. Mukherji, "Novel U-bent fiber optic probe for localized surface plasmon resonance based biosensor," *Biosensors & Bioelectronics*, 2009, 24(9): 2804–2809.

[49] S. Chauhan, N. Punjabi, D. Sharma, and S. Mukherji, "Evanescent wave absorption based S-shaped fiber-optic biosensor for immunosensing applications," *Procedia Engineering*, 2016, 168: 117–120.

[50] S. K. Chauhan, J. Tharion, N. Punjabi, D. K. Sharma, and S. Mukherji, "A comparison of S-shaped and U-shaped optical fiber sensors," *Optical Sensors*,

2014: SeTh3B.5.

[51] Z. W. Luo, Y. Xu, L. He, F. He, J. Wu, Z. J. Huang, *et al.*, "Development of a rapid and ultra-sensitive cytosensor: Ω-shaped fiber optic LSPR integrated with suitable AuNPs coverage," *Sensors and Actuators B: Chemical*, 2021, 336: 129706.

[52] Y. Li, X. Wang, W. Ning, E. L. Yang, Y. X. Li, Z. W. Luo, *et al.*, "Sandwich method-based sensitivity enhancement of Ω-shaped fiber optic LSPR for time-flexible bacterial detection," *Biosensors & Bioelectronics*, 2022, 201: 113911.

[53] L. He, F. He, Y. T. Feng, X. Wang, Y. X. Li, Y. H. Tian, *et al.*, "Hybridized nanolayer modified Ω-shaped fiber-optic synergistically enhances localized surface plasma resonance for ultrasensitive cytosensor and efficient photothermal therapy," *Biosensors & Bioelectronics*, 2021, 194: 113599.

[54] P. Dimpi and R. Biswas, "Clad modified varying geometries of fiber optic LSPR sensors towards detection of hazardous volatile liquids and their comparative analysis," *Environmental Technology & Innovation*, 2022, 25: 102112.

[55] J. K. Virk, S. Das, R. S. Kaler, H. Singh, and T. Kundu, "D-shape optical fiber probe dimension optimization for LSPR based bio-sensor," *Optical Fiber Technology*, 2022, 71: 102903.

[56] A. K. Pathak, B. M. A. Rahman, V. K. Singh, and S. Kumari, "Sensitivity enhancement of a concave shaped optical fiber refractive index sensor covered with multiple Au nanowires," *Sensors*, 2019, 19(19): 4021.

[57] J. B. Maurya, Nikki, J. P. Saini, A. K. Sharma, and Y. K. Prajapati, "A localized SPR D-shaped fiber optic sensor utilizing silver grating coated with graphene: Field analysis," *Optical Fiber Technology*, 2023, 75: 103204.

[58] J. Feng, J. Gao, W. Yang, R. Liu, M. Shafi, Z. Zha, *et al.*, "LSPR optical fiber sensor based on 3D gold nanoparticles with monolayer graphene as a spacer," *Optics Express*, 2022, 30(6): 10187–10198.

[59] Q. Yang, X. Zhang, S. Kumar, R. Singh, B. Zhang, C. Bai, *et al.*, "Development of glucose sensor using gold nanoparticles and glucose-oxidase functionalized tapered fiber structure," *Plasmonics*, 2020, 15(3): 841–848.

[60] J. Cao, M. H. Tu, T. Sun, and K. T. V. Grattan, "Wavelength-based localized surface plasmon resonance optical fiber biosensor," *Sensors and Actuators B: Chemical*, 2013, 181: 611–619.

[61] J. G. Ortega-Mendoza, A. Padilla-Vivanco, C. Toxqui-Quitl, P. Zaca-Morán, D. Villegas-Hernández, and F. Chávez, "Optical fiber sensor based on localized surface plasmon resonance using silver nanoparticles photodeposited on the optical fiber end," *Sensors*, 2014, 14(10): 18701–18710.

[62] V. T. Huong, N. T. T. Phuong, N. T. Tai, N. T. An, V. D. Lam, D. H. Manh, *et al.*, "Gold nanoparticles modified a multimode clad-free fiber for ultrasensitive detection of bovine serum albumin," *Journal of Nanomaterials*, 2021, 2021: 1–6.

[63] U. M. Uh, J. S, Kim, J. H. Park, J. D. H. Leong, H. Y. Lee, S. M. Lee, *et al.*, "Fabrication of localized surface plasmon resonance sensor based on optical fiber and micro fluidic channel," *Journal of Nanoscience and Nanotechnology*, 2017, 17(2): 1083–1091.

[64] Y. Shao, S. Xu, X. Zheng, Y. Wang, and W. Xu, "Optical fiber LSPR biosensor prepared by gold nanoparticle assembly on polyelectrolyte multilayer," *Sensors*, 2010, 10(4): 3585–3596.

[65] H. M. Kim, D. H. Jeong, H. Y. Lee, J. H. Park, and S. K. Lee, "Improved stability of gold nanoparticles on the optical fiber and their application to refractive index sensor based on localized surface plasmon resonance," *Optics and Laser Technology*, 2019, 114: 171–178.

[66] M. D. Lu, H. Zhu, C. G. Bazuin, W. Peng, and J. F. Masson, "Polymer-templated gold nanoparticles on optical fibers for enhanced-sensitivity localized surface plasmon resonance biosensors," *ACS Sensors*, 2019, 4(3): 613–622.

[67] M. D. Lu, H. Zhu, M. Lin, F. Wang, L. Hong, J. F. Masson, *et al.*, "Comparative study of block copolymer-templated localized surface plasmon resonance optical fiber biosensors: CTAB or citrate-stabilized gold nanorods," *Sensors and Actuators B: Chemical*, 2021, 329: 129094.

[68] M. D. Lu, H. Zhu, L. Hong, J. J. Zhao, J. F. Masson, and W. Peng, "Wavelength-tunable optical fiber localized surface plasmon resonance biosensor via a diblock copolymer-templated nanorod monolayer," *ACS Applied Materials & Interfaces*, 2020, 12(45): 50929–50940.

[69] H. Nguyen, F. Sidiroglou, S. F. Collins, T. J. Davis, A. Roberts, and G. W. Baxter, "A localized surface plasmon resonance-based optical fiber sensor with sub-wavelength apertures," *Applied Physics Letters*, 2013, 103(19): 607.

[70] H. M. Kim, M. Uh, D. H. Jeong, H. Y. Lee, J. H. Park, and S. K. Lee, "Localized surface plasmon resonance biosensor using nanopatterned gold particles on the surface of an optical fiber," *Sensors and Actuators B: Chemical*, 2019, 280: 183–191.

[71] Y. Hong, D. Zhao, J. Wang, J. Lu, G. Yao, D. Liu, *et al.*, "Solvent-free nanofabrication based on ice-assisted electron-beam lithography," *Nano Letters*, 2020, 20(12): 8841–8846.

[72] H. M. Kim, K. T. Nam, S. K. Lee, and J. H. Park, "Fabrication and measurement of microtip-array-based LSPR sensor using bundle fiber," *Sensors and Actuators A: Physical*, 2018, 271: 146–152.

[73] H. H. Jeong, N. Erdene, J. H. Park, D. H. Jeong, H. Y. Lee, and S. K. Lee, "Real-time label-free immunoassay of interferon-gamma and prostate-

specific antigen using a fiber-optic localized surface plasmon resonance sensor," *Biosensors & Bioelectronics*, 2013, 39(1): 346–351.

[74] H. M. Kim, H. J. Kim, J. H. Park, and S. K. Lee, "High-performance biosensor using a sandwich assay via antibody-conjugated gold nanoparticles and fiber-optic localized surface plasmon resonance," *Analytica Chimica Acta*, 2022, 1213: 339960.

[75] S. Das, B. Mandal, V. R. Rao, and T. Kundu, "Detection of tomato leaf curl New Delhi virus DNA using U-bent optical fiber-based LSPR probes," *Optical Fiber Technology*, 2022, 74: 103108.

[76] T. Endo, K. Kerman, N. Nagatani, Y. Takamura, and E. Tamiya, "Label-free detection of peptide nucleic acid-DNA hybridization using localized surface plasmon resonance based optical biosensor," *Analytical Chemistry*, 2005, 77(21): 6976–6984.

[77] D. Zhang, Y. Yan, Q. Li, T. Yu, W. Cheng, L. Wang, *et al.*, "Label-free and high-sensitive detection of Salmonella using a surface plasmon resonance DNA-based biosensor," *Journal of Biotechnology*, 2012, 160(3–4): 123–128.

[78] F. Tukur, B. Bagra, A. Jayapalan, M. Liu, P. Tukur, and J. Wei, "Plasmon-exciton coupling effect in nanostructured arrays for optical signal amplification and SARS-CoV-2 DNA sensing," *ACS Applied Nano Materials*, 2023, 6(3): 2071–2082.

[79] W. Ning, C. Y. Zhang, Z. Y. Tian, M. F. Wu, Z. W. Luo, S. M. Hu, *et al.* "Ω-shaped fiber optic LSPR biosensor based on mismatched hybridization chain reaction and gold nanoparticles for detection of circulating cell-free DNA," *Biosensors & Bioelectronics*, 2023, 228: 115175.

[80] M. D. Lu, W. Peng, M. Lin, F. Wang, and Y. Zhang, "Gold nanoparticle-enhanced detection of DNA hybridization by a block copolymer-templating fiber-optic localized surface plasmon resonance biosensor," *Nanomaterials*, 2021, 11(3): 616.

[81] L. Hong, M. D. Lu, M. P. Dinel, P. Blain, W. Peng, H. Y. Gu, *et al.*, "Hybridization conditions of oligonucleotide-capped gold nanoparticles for SPR sensing of microRNA," *Biosensors & Bioelectronics*, 2018, 109: 230–236.

[82] S. Y. Qian, M. Lin, W. Ji, H. Z. Yuan, Y. Zhang, Z. G. Jing, *et al.*, "Boronic acid functionalized Au nanoparticles for selective microRNA signal amplification in fiber-optic surface plasmon resonance sensing system," *ACS Sensors*, 2018, 3(5): 7b00871.

[83] Z. Luo, Y. Wang, Y. Xu, X. Wang, Z. Huang, J. Chen, *et al.*, "Ultrasensitive U-shaped fiber optic LSPR cytosensing for label-free and in situ evaluation of cell surface N-glycan expression," *Sensors and Actuators B: Chemical*, 2019, 284: 582–588.

[84] Y. Xu, Z. Luo, J. Chen, Z. Huang, X. Wang, H. An,

et al., "Ω-shaped fiber-optic probe-based localized surface plasmon resonance biosensor for real-time detection of salmonella typhimurium," *Analytical Chemistry*, 2018, 90(22): 13640–13646.

[85] S. Kumar, Z. Guo, R. Singh, Q. L. Wang, B. Y. Zhang, S. Cheng, *et al.*, "MoS₂ functionalized multicore fiber probes for selective detection of shigella bacteria based on localized plasmon," *Journal of Lightwave Technology*, 2021, 39(12): 4069–4081.

[86] W. Ning, S. Hu, C. Zhou, J. Luo, Y. Li, C. Zhang, *et al.*, "An ultrasensitive J-shaped optical fiber LSPR aptasensor for the detection of Helicobacter pylori," *Analytica Chimica Acta*, 2023, 1278: 341733.

[87] S. K. Srivastava, V. Arora, S. Sapra, and B. D. Gupta, "Localized surface plasmon resonance-based fiber optic U-shaped biosensor for the detection of blood glucose," *Plasmonics*, 2012, 7(2): 261–268.

[88] S. Jia, C. Bian, J. Z. Sun, J. H. Tong, and S. H. Xia, "A wavelength-modulated localized surface plasmon resonance (LSPR) optical fiber sensor for sensitive detection of mercury(II) ion by gold nanoparticles-DNA conjugates," *Biosensors & Bioelectronics*, 2018, 114: 15–21.

[89] Y. C. Xu, M. Xiong, and H. Yan, "A portable optical fiber biosensor for the detection of zearalenone based on the localized surface plasmon resonance," *Sensors and Actuators B: Chemical*, 2021, 336: 129752.

[90] B. B. Luo, Y. J. Wang, H. F. Lu, S. X. Wu, Y. M. Lu, S. H. Shi, *et al.*, "Label-free and specific detection of soluble programmed death ligand-1 using a localized surface plasmon resonance biosensor based on excessively tilted fiber gratings," *Biomedical Optics Express*, 2019, 10(10): 5136–5148.

[91] G. Liang, Z. Zhao, Y. Wei, K. Liu, W. Hou, and Y. Duan, "Plasma enhanced label-free immunoassay for alpha-fetoprotein based on a U-bend fiber-optic LSPR biosensor," *RSC Advances*, 2015, 5(31): 23990–23998.

[92] H. M. Kim, D. H. Jeong, H. Y. Lee, J. H. Park, and S. K. Lee, "Improved stability of gold nanoparticles on the optical fiber and their application to refractive index sensor based on localized surface plasmon resonance," *Optics and Laser Technology*, 2019, 114: 171–178.

[93] M. Sanders, Y. B. Lin, J. J. Wei, T. Bono, and R. G. Lindquist, "An enhanced LSPR fiber-optic nanoprobe for ultrasensitive detection of protein biomarkers," *Biosensors & Bioelectronics*, 2014, 61: 95–101.

[94] P. Halkare, N. Punjabi, J. Wangchuk, S. Madugula, K. Kondabagil, and S. Mukherji, "Label-free detection of Escherichia coli from mixed bacterial cultures using bacteriophage T4 on plasmonic fiber-optic sensor," *ACS Sensors*, 2021, 6(7): 2720–2727.

[95] S. Kumar, R. Singh, B. K. Kaushik, N. K. Chen, Q. S. Yang, and X. Zhang, "LSPR-based cholesterol biosensor using hollow core fiber structure," *IEEE Sensors Journal*, 2019, 19(17): 7399–7406.

[96] S. Kumar, R. Singh, Q. S. Yang, S. Cheng, B. Y. Zhang, and B. K. Kaushik, "Highly sensitive, selective and portable sensor probe using germanium-doped photosensitive optical fiber for ascorbic acid detection," *IEEE Sensors Journal*, 2021, 21(1): 62–70.

[97] M. Y. Li, R. Singh, C. Marques, B. Y. Zhang, and S. Kumar, "2D material assisted SMF-MCF-MMF-SMF based LSPR sensor for creatinine detection," *Optics Express*, 2021, 29(23): 38150–38167.

[98] Q. S. Yang, G. Zhu, L. Singh, Y. Wang, R. Singh, B. Y. Zhang, *et al*., "Highly sensitive and selective sensor probe using glucose oxidase/gold nanoparticles/graphene oxide functionalized tapered optical fiber structure for detection of glucose," *Optik*, 2020, 208: 164536.